THE USE OF N-POLYETHEREAL POLYPYRROLES IN PRECONCENTRATION AND SURFACE ENHANCED RAMAN SCATTERING STUDIES

A THESIS SUBMITTED TO
THE GRADUATE SCHOOL OF NATURAL AND APPLIED SCIENCES
OF
MIDDLE EAST TECHNICAL UNIVERSITY

BY

BAHAR KÖKSEL

IN PARTIAL FULFILLMENT OF THE REQUIREMENTS
FOR
THE DEGREE OF MASTER OF SCIENCE
IN
CHEMISTRY

FEBRUARY 2009

Approval of the thesis:

THE USE OF N-POLYETHEREAL POLYPYRROLES IN PRECONCENTRATION AND SURFACE ENHANCED RAMAN SCATTERING STUDIES

submitted by **BAHAR KÖKSEL** in partial fulfillment of the requirements for the degree of **Master of Science in Chemistry Department, Middle East Technical University** by,

Prof. Dr. Canan Özgen
Dean, Graduate School of **Natural and Applied Sciences** _____

Prof. Dr. Ahmet M. Önal
Head of Department, **Chemistry** _____

Prof. Dr. Mürvet Volkan
Supervisor, **Chemistry Dept., METU** _____

Examining Committee Members:

Prof. Dr. O. Yavuz Ataman
Chemistry Dept., METU _____

Prof. Dr. Mürvet Volkan
Chemistry Dept., METU _____

Prof. Dr. E. Hale Göktürk
Chemistry Dept., METU _____

Prof. Dr. Ahmet M. Önal
Chemistry Dept., METU _____

Assoc. Prof. Dr. Atilla Cihaner
Chemistry Group, Atılım University _____

Date: February 23, 2009

I hereby declare that all information in this document has been obtained and presented in accordance with academic rules and ethical conduct. I also declare that, as required by these rules and conduct, I have fully cited and referenced all material and results that are not original to this work.

Name, Last name: Bahar, Köksel

Signature :

ABSTRACT

THE USE OF N-POLYETHEREAL POLYPYRROLES IN PRECONCENTRATION AND SURFACE ENHANCED RAMAN SCATTERING STUDIES

Köksel, Bahar

M.S., Department of Chemistry

Supervisor: Prof. Dr. Mürvet Volkan

February 2009, 61 pages

Polypyrroles containing polyether pseudocages (P**I**, P**II**, P**III**) have been synthesized via chemical oxidation of 1,5-bis(1,1-pyrrole)-3-oxabutane (M**I**), 1,8-bis(1,1-pyrrole)-3,6-dioxahexane (M**II**), and 1,11-bis(1,1-pyrrole)- 3,6,9-trioxaundecane (M**III**) using anhydrous $FeCl_3$ in $CHCl_3$. Because as obtained polymer resins did not give any response toward any cations, they were reduced (undoped) using chemical reducing agents. Tetrabutylammonium hydroxide (TBAOH) was found to be more effective in undoping to obtain more reproducible and reusable polymer resins. It was investigated whether the undoped polymer resins were used for the extraction of rare earth metal ions from the aqueous medium. Among them, only P**III** resin can extract La(III), Eu(III) and Yb(III) from their aqueous solutions and can be employed for the preconcentration of these metal ions. For batch extraction of La(III), Eu(III) and Yb(III) at neutral pH values, percent recoveries of 98.0, 90.7 and 87.3, respectively, has been obtained by using Inductively Coupled Plasma Optical

Emission Spectroscopy (ICP-OES) technique. The sorption capacity is found as 1.3 mg of La(III) per gram of P**III** resin. The P**III** resin could be reused at least five times without significant change in its sorption capacity. P**III** has also been synthesized via electrochemical method to be used in the preparation of Surface Enhanced Raman Scattering (SERS) active substrate. P**III** has been polymerized on Indium Tin Oxide (ITO) glass by using constant potential electrolysis. In an electrolyte solution containing 0.05M tetrabutylammonium perchlorate (TBAP), 1.2 V vs. Ag wire (oxidation potential of M**III**) was applied for coating and then silver particles were deposited on the surface of P**III** coated ITO electrode by reducing Ag(I) in monomer free electrolyte solution electrochemically. As an alternative, another SERS substrate was prepared electrochemically by depositing silver particles directly on ITO glass. The performances of prepared ITO-P**III-**Ag and ITO-Ag SERS substrates were evaluated with dilute solutions of brilliant cresyl blue (BCB), crystal violet (CV), para amino benzoic acid (PABA), nicotine and nicotinic acid.

Keywords: SERS, Preconcentration, Polypyrrole, Polyether Pseudocages, Rare Earth Ions.

ÖZ

N-POLİETERİK POLİPİROLLERİN ÖN ZENGİNLEŞTİRME VE YÜZEYDE GÜÇLENDİRİLMİŞ RAMAN SAÇILMASI ÇALIŞMALARINDA KULLANIMI

Köksel, Bahar

Yüksek Lisans, Kimya Bölümü

Tez Yöneticisi: Prof. Dr. Mürvet Volkan

Şubat 2009, 61 sayfa

Polieter köprülü (P**I**, P**II**, P**III**) polipiroller, $CHCl_3$ içinde susuz $FeCl_3$ kullanılarak 1,5-bis(1,1-pirol)-3-oksabütan (M**I)**, 1,8-bis(1,1-pirol)-3,6-dioksaheksan (M**II)** ve 1,11-bis(1,1-pirol)-3,6,9-trioksaundekan (M**III**)' ün kimyasal olarak yükseltgenmesiyle sentezlenmiştir. Sentezlenen reçineler herhangi bir katyona karşı tepki vermediğinden kimyasal indirgenler kullanılarak indirgenmiştir. Tetrabütilamonyum hidroksit (TBAOH) ile indirgenen polimerlerin tekrar edilebilirlik ve tekrar kullanılabilirlik açısından daha etkili olduğu gözlenmiştir. İndirgenmiş polimer reçineler nadir toprak metal iyonlarının sulu ortamdan ekstraksiyonu için denenmiştir. Aralarında sadece P**III** reçine La(III), Eu(III) ve Yb(III) iyonlarını sulu çözeltiden alabilmekte olup önzenginleştirme için kullanılabilir. P**III** reçine kullanılarak nötral pH değerlerinde gerçekleştirilen tekne (Batch) tipi ekstraksiyon çalışmalarında La(III), Eu(III) ve Yb(III)'ün yüzde geri kazanımlarının sırasıyla 98.0, 90.7 ve 87.3 olduğu İndüktif Eşleşmiş Plazma Optik Emisyon Spektroskopi (ICP-OES) tekniği ile saptanmıştır. P**III** reçinenin

La(III) iyonu için önzenginleştirme kapasitesi 1.3 mg La(III) / g reçine olarak bulunmuştur. P**III** reçine geri kazanımda önemli bir fark olmaksızın en az beş defa ard arda kullanılmıştır. P**III** yüzeyde güçlendirilmiş Raman saçılması aktif yüzey hazırlanmasında kullanılmak üzere elektrokimyasal olarak da sentezlenmiştir. M**III** indiyum-kalay oksit (ITO) cam üzerine Ag tele karşı 1.2 V (M**III**' ün yükseltgenme potansiyeli) uygulanarak 0.05 M tetrabütilamonyum per klorat (TBAP) içeren elektrolit çözeltisi içinde sabit potansiyel elektroliz yöntemi ile polimerleştirildikten sonra Ag(I), P**III** ile kaplanmış ITO elektrot yüzeyinde metalik gümüşe indirgenmiş ve gümüş parçacıklar oluşturulmuştur. Bu yüzeye alternatif olarak diğer bir yüzey hazırlanmış ve bu çalışmada gümüş parçacıklar doğrudan doğruya ITO cam yüzey üzerine elektrokimyasal olarak toplanmıştır. Hazırlanan ITO-P**III-**Ag ve ITO-Ag SERS yüzeylerinin performansları parlak krezil mavisi (BCB), kristal menekşe (CV), para amino benzoik asit (PABA), nikotin ve nikotinik asitin düşük derişimlerdeki çözeltileri kullanılarak değerlendirilmiştir.

Anahtar Kelimeler: Ön zenginleştirme, Polipirol, Polieter Köprü, Nadir Toprak İyonları.

To My Grandfather,

ACKNOWLEDGEMENTS

I would like to express my feelings of gratitude and appreciation to my supervisor Prof. Dr. Mürvet Volkan for her guidance, advice, criticism, encouragements and support throughout the study.

I would like to thank to Prof. Dr. Ahmet M. Önal for his guidance, support, and contribution throughout the study.

I am also deeply grateful to Assoc. Prof. Dr. Atilla Cihaner for his guidance, support and advice during all my study.

My special thanks to Murat Kaya and Seher Karabıçak for their continuous help in my work, their valuable discussions and their friendship.

I want to thank to my labmates Rukiye Sancı, Seda Kibar and Nehir Güler, and all C-50 and B-24 lab members for their friendship and kind support.

I also give my thanks to my friends Ayşe Aybey, Asuman Aybey and Deniz Çağlar Özyaşar encouraged me at the beginning of my M.S study and their warm friendship.

Finally, my special appreciation and gratitude is devoted to my mother, my father and my brother for their trust, patience and moral support, which makes everything possible.

TABLE OF CONTENTS

LIST OF TABLES

TABLES

LIST OF FIGURES

FIGURES

LIST OF ABBREVIATIONS

ABBREVIATIONS

Surface Enhanced Raman Scattering	SERS
Poly-1,5-bis(1,1-pyrrole)-3-oxabutane	P**I**
Poly-1,8- bis(1,1-pyrrole)-3,6-dioxahexane	P**II**
Poly-1,11-bis(1,1-pyrrole)- 3,6,9-trioxaundecane	P**III**
Brillant Cresyl Blue	BCB
Crystal Violet	CV
Para amino benzoic acid	PABA
Tetrabutylammonium hydroxide	TBAOH
Inductively Coupled Plasma Optical Emission Spectroscopy	ICP-OES
Indium Tin Oxide	ITO
Tetrabutylammonium perchlorate	TBAP
Rare Earth Elements	REEs
Field Emission Scanning Electron Microscopy	FE-SEM

CHAPTER 1

INTRODUCTION

1.1 Preconcentration Studies

1.1.1 Polyethereal Polymer Resin

Conducting polymers functionalized with crown ethers and polyether pseudo-cages have been a center of interest due to their complexing properties towards alkaline and alkaline earth metal cations; hence such molecules and their polymers are good exchanger for metallic cations [1].

The selective binding of guest molecules to conducting polymers can be a suitable approach for the extraction of cations. However, most of the polymers with crown ether appendages have solubility problems and water incompatibility and also it is difficult to synthesize such polymers. Therefore, only few studies reported.

Some polyethereal polymers of this type are shown in Figure 1.1. Azocrown ether substituted polymer **3** shown in Figure 1.1. had minor voltammetric response toward Na^+ and K^+ in organic medium; unfortunately, the replacement of Li^+ by those ions was found to be irreversible [2].

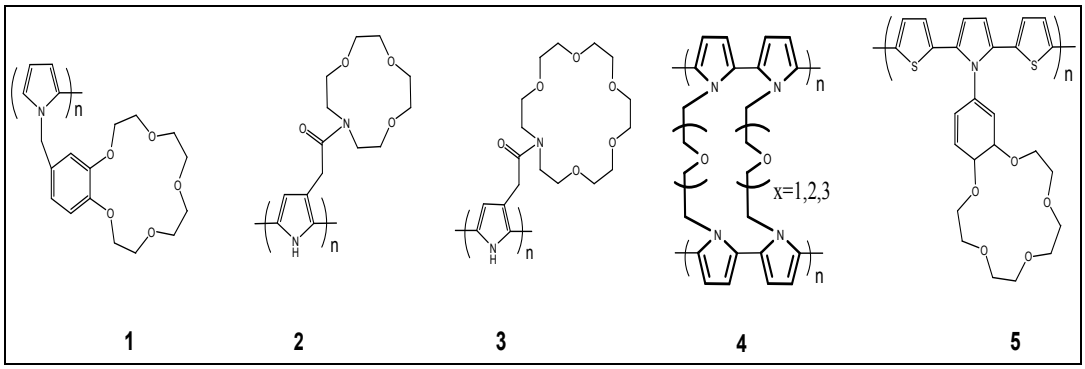

Figure 1.1. Polyethereal polymers with pyrrole backbones.

Recently, Cihaner and Algı [3] have synthesized polymer **5** shown in Figure 1.1 and they have observed that polymer **5** has more effective complexing properties towards alkaline metal cations as compared with polymer **1**, **2** and **3** [4, 5].

Very recently, Simonet and co-workers have synthesized monomers containing two pyrrolyl units linked by the different length of polyether chains this is shown in Figure 1.1 as the compound **4** [2]. Macrocyclic cavities could be achieved via anodic polymerization; however, for the large scale synthesis of the polymer **4** an industrial type cell was needed. The complexing properties of such polymers have been investigated and a strong affinity toward Co^{2+}, Cs^{+}, K^{+}, and Ag^{+} cations was reported.

Recently, Cihaner synthesized N-polyethereal polypyrroles **4** via electrochemical polymerizaton and its copolymers with pyrrole (Figure 1.1) [1, 6].

1.1.2 Rare Earth Elements (REEs)

The lanthanides classified as Rare Earth Elements (REEs) are located in block 5*d* of the periodic table (Figure 1.2). Although in fact they are not all rare, the close similarity of their chemical and physical properties made the occurrence of several of them together in individual minerals almost inevitable. Several of the lanthanides form during the fission of uranium and plutonium [7, 8].

REEs can be classified in three groups; the light, the heavy and the middle groups. Although these terms are imprecise, they are very convenient; by light earths the elements from lanthanum, cerium, praseodymium, neodymium, promethium, samarium are meant; similarly the heavy earths comprise erbium, thulium, ytterbium, lutetium; and the middle earth's europium, gadolinium, terbium, dysprosium, holmium.

Figure 1.2. Lanthanide Series.

The lanthanides have many scientific and industrial uses. Their compounds are used as catalysts in the production of petroleum and synthetic products. Lanthanides are used in lamps, lasers, magnets, phosphors, motion picture projectors, and X-ray intensifying screens. A pyrophoric mixed rare-earth alloy called Mischmetall (50% Ce, 25% La, 25% other light lanthanides) or misch metal is combined with iron to make flints for cigarette lighters [8].

As a result of their usage, more and more REEs are getting into the environment, accumulating in natural waters, soils and then entering into the food chain. Continuous exposure to low or high concentrations of REEs could cause adverse health effects. Their effect on environmental ecosystem has also been the subject of continual attention. Sometimes, natural water system becomes the ‘‘source’’ and ‘‘influx’’ of metal ions among the cycle of environmental ecosystem. Therefore, developing sensitive and accurate methods to determine REEs in natural water is necessary [9].

1.1.3 Preconcentration Methods of REEs

In environmental samples, the concentration of the element to be determined may be below the detection limit of the measurement technique, and thus a preconcentration step is required. Analytical techniques are then applied after a preconcentration step.

Preconcentration is a process in which the ratio of the amount of a desired trace element to that of the original matrix is enhanced. Preconcentration improves the analytical detection limit, increases the sensitivity sometimes by several orders of magnitude, enhances the accuracy of the results and facilitates easy calibration [10]. The enrichment techniques generally employed for the REEs are liquid–liquid extraction, solid phase extraction and coprecipitation.

Liquid liquid extraction is based on the distribution of a solute between two immiscible solvents.

Xu et al. studied a direct sampling with organic solvent extracts for simultaneous multi-element determination implemented with inductively coupled plasma atomic emission spectrometry associated with a flow injection liquid-liquid extraction sample preconcentration method [11].

Agrawal et al. used N-phenyl-(1,2-methanofullerene C_{60})61-formohydroxamic acid (Figure 1.3) for the liquid-liquid extraction and separation of cerium and lanthanum from monazite sands in the presence of diverse ions in high purity (99.98%) [12].

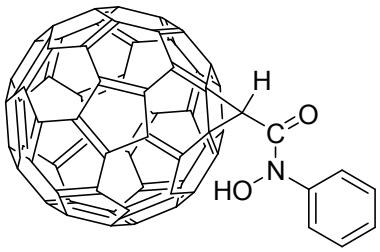

Figure 1.3. N-phenyl-(1,2-methanofullerene C60)61-formohydroxamic acid.

Co-precipitation is the process of carrying down of analyte along with the co-precipitant under the conditions of preconcentration or surface absorption.

Taicheng et al. carried a study with the $Ti(OH)_4$-$Fe(OH)_3$ co-precipitation system, and the results obtained showed that the natural situation of Ti tightly coexisting with Nb, Ta, Zr, and Hf in geological samples plays a very important role in the complete co-precipitation of the four elements [13].

The basic principle of solid phase extraction or solid-liquid extraction is the transfer of analyte from aqueous phase to the active sites of the adjacent solid phase. This transfer is stimulated by the selection of appropriate operational conditions in the system of three major components liquid phase, analyte, and sorbent [10].

Agrawal has synthesized a new fullerene derivative poly(b-styryl)-(1,2-methanofullerene-C60)61- formohydroxamic acid (Figure 1.4) and which was applied for the solid phase extraction, separation, preconcentration and ICP-MS determination of Ce, La, Pr, Nd, Sm and Gd. Introduction of the fullerene moiety into poly(b-styryl)-hydroxamic acid enhances its reactivity, chemical stability and recycled for their determination [14].

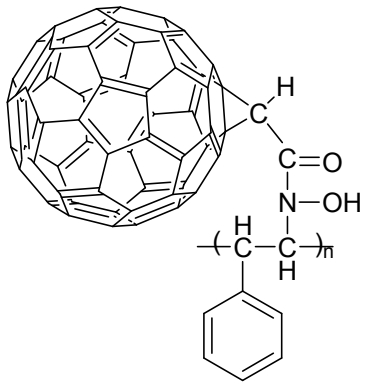

Figure 1.4. Poly(b-styryl)-(1,2-methanofullerene-C60)61- formohydroxamic acid.

Fu et al. used a newly synthesized alkyl phosphinic acid resin (APAR) (Figure 1.5) as a solid phase for on-line preconcentration of trace REEs (lanthanides including yttrium) and then determined by inductively coupled plasma mass spectrometry [15].

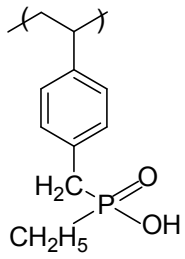

Figure 1.5. Alkyl phosphinic acid resin.

Chen et al. have used carbon nanofibers first time for the preconcentration of rare earths. They have successfully applied for determination of light (La), medium (Eu and Gd) and heavy (Yb) REEs in real sample with the recovery more than 90% [16].

The cross-linked chitosan functionalized with 2-amino-5- hydroxy benzoic acid moiety (CCTS-AHBA resin) was prepared by Sabarudin et. al. (Figure 1.6) for the determination of 24 trace rare elements such as Ag, Be, Cd, Co, Cu, Ni, Pb, U, V, and REEs in water samples [17].

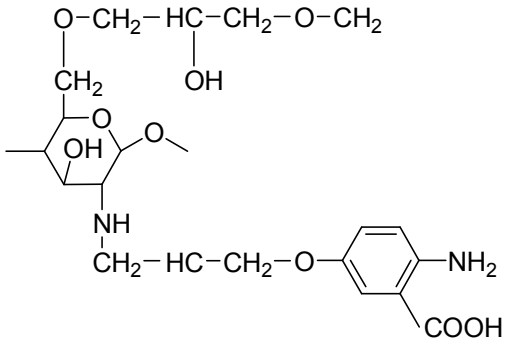

Figure 1.6. CCTS-AHBA, cross-linked chitosan possessing 2-amino-5-hydroxy benzoic acid moiety.

Between these preconcentration techniques, ion exchange is one of the most common, most practical and most extensively used methods. Thus in this study, N-polyetheral polypyrroles were synthesized and used as an ion exchange resin.

1.1.3.1 Ion Exchange

Organic polymers have been used as ion exchange resins for a long time. Ion exchange involves exchange of ions of like sign between a solution and a solid of highly insoluble body in contact with it. Analyte of interest can be exchangedfrom dilute solution with resin by either batch or column mode of operation. Subsequently the analyte is eluated with a small volume, thus resulting in preconcentration. Later the ion exchange resin can be regenerated with a proper electrolyte solution. The capacity of ion exchangers is defined in terms of the number of exchangeable counter ions in the resin [18].

There are different types of ion exchange resins, which are fabricated to selectively prefer one or several different types of ions. For example, Korsakova et al. [19] determined ultra trace REEs in sulfide minerals by using cation exchange resin Dowex 50W-X8 by ICP-MS method. The detection limit was found 0.06ng/g for lutetium and 0.05 ng/g for cerium.

Pasinli et al. used different ion exchanger Amberlite CG-120, Amberlite IR-120, Rexyn 101, Dowex 50W X18 for REEs and determined La, Eu and Yb in natural water samples by using ICP-OES [20].

Kong et al. used on-line procedure for preconcentration and determination of cobalt and nickel at low concentration levels by microwave plasma torch-atomic emission spectrometry (MPT-AES) using a minicolumn packed with type 732 cation exchange resin [21].

1.1.4 Analytical Techniques for Determination of REEs

With the rising use of the REEs in industry, determination of the REEs is gaining importance. The precise determination of these elements is therefore very important. There have been many analytical techniques used for the determination of REEs in solid and solution samples; which are neutron activation analysis (NAA) [22-23], isotope dilution mass spectrometry (IDMS) [24], inductively coupled plasma optical emission spectrometry (ICP-OES), and inductively coupled plasma mass spectrometry (ICP-MS) [25].

Among them, plasma methods provide some of the most useful and specific means for the determination of the REEs at trace levels. Even though the chemical properties of various lanthanides are very similar, the spectra of these elements are just as unique as those of other elements [26].

1.1.4.1 Inductively Coupled Plasma Optical Emission Spectroscopy (ICP-OES)

It is an analytical technique used for the detection of trace metals. It is a type of emission spectroscopy that uses the inductively coupled plasma to produce excited atoms and ions that emit electromagnetic radiation at wavelengths characteristic of a particular element [27, 28].

The intensity of this emission is indicative of the concentration of the element within the sample. In principle, all metallic elements can be determined by plasma emission spectrometry. High sensitivity, multi element analysis capability, speed of analysis and high reproducibility are the advantages of ICP-OES technique. Having high energy, ICP permits the determination of elements that tend to form refractory compounds that is compounds that are highly resistant to decomposition by heat [26].

After solid-liquid extraction with microcrystalline naphthalene, Cai et al. determined lanthanum, europium and ytterbium by using ICP-OES and detection limits of this method for La(III), Eu(III) and Yb(III) were within 1.3–8.6 ng mL^{-1}[29].

Liang et al. firstly prepared a new chelating resin silica gel loaded with 1-phenyl-3-methyl-4-benzoylpyrazol-5-one, and used this resin for the preconcentration of trace amounts of REEs (La, Eu and Yb) in water samples prior to their determination by ICP-OES. The adsorption capacity of modified silica gel for La, Eu and Yb was 0.208, 0.249 and 0.239 mmol g^{-1}, respectively [30].

Hang et al. determined Sm, Tm, Ho, and Nd in geological samples by ICP-OES. The technique was based on adsorption of analytes on Nanometer-Size Titanium Dioxide (NSTD) packed in a microcolumn and separation from the matrix at pH = 7.0. At a flow rate of 1.0 mL min^{-1}, the detection limits (3s) of the technique for

Tm, Sm, Ho, and Nd with an enrichment factor of 50 were 0.06, 0.18, 0.08, and 0.1 ng mL^{-1}, and the RSD were 1.8%, 4.7%, 2.0%, and 1.6%, respectively [31].

Cao et. al. developed a method for the determination of trace REEs based on preconcentration with a microcolumn packed with immobilized nanometer TiO_2 and determination by ICP-OES. The detection limits for REEs was between 3 and 57 ng L^{-1} [32].

1.2 Surface Enhanced Raman Scattering (SERS) Studies

1.2.1 SERS

Raman scattering is an inelastic photon scattering which was first witnessed by C. V. Raman. He received Nobel Prize in 1930 for the discovery of Raman Effect.

There are two types of scattering. The first one is elastic scattering, which is known as Rayleigh scattering. In this type of scattering there is no energy change between incident photons and molecules and hence there is no Raman Effect. In the second type, scattering molecule can absorb energy or lose energy that is known as inelastic scattering and this type of scattering is named as Raman Scattering.

Until the discovery of SERS effect in 1970's Raman was an unpractical technique because approximately one photon is in elastically scattered for every 10^{10} elastically scattered photons. In the 1970s, a discovery, which showed unexpectedly high Raman signals (Figure 1.7) from pyridine on a rough silver electrode surface, attracted considerable attention [33].

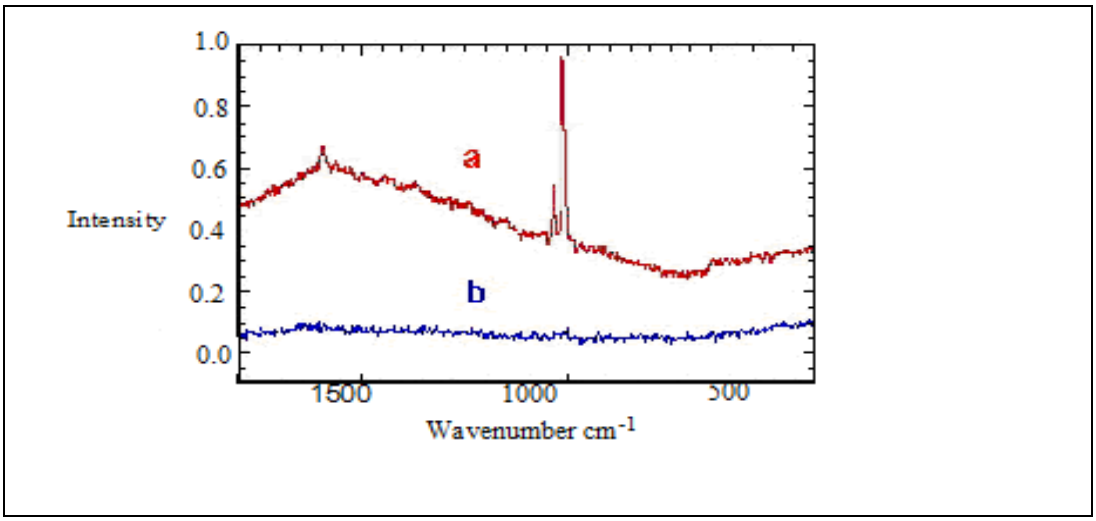

Figure 1.7. Typical Raman Shifts Pyridine Aqueous Solution a) SERS spectrum of 2.5 mM pyridine solution**,** b) Normal Raman Scattering spectrum of 63 mM pyridine solution.

This experiment shows that SERS increases the Raman intensity of a molecule via plasmonic phenomenon whereby molecules at or near a noble metal surface with nanoscale structural features. SERS can increase the Raman intensity of a molecule in proximity to a nanoscale roughened surface by 10^8 [34].

The electromagnetic enhancement is a consequence of the interaction of the incident electric field (from the incident radiation) with electrons in the metal surface, which cause excitation of surface plasmons (collective oscillations of metal electrons) and, as a result, enhancement of the electric field at the metal surface. Excitation of surface plasmons at smooth surfaces is usually not possible (because of mismatch of the momentum of the photon and that of the surface plasmon); therefore, metal substrates for SERS measurements should be rough [35].

Mechanism responsible for enhancement in Raman intensity has not yet been completely explained. In addition to a long-range classical electromagnetic (EM) effect arised from the surface plasmon resonance there is another effect that is a

short-range chemical (CHEM) effect related to active sites or charge transfer processes have been proposed as contributors in the overall surface enhancement [36, 37].

1.2.2 Surface Enhanced Raman Active Substrates

SERS represented a great advance in the field of the Raman spectroscopy during the seventies since the inherent weakness of the Raman signal can be substantially increased by six or more orders of magnitude [38].

The application of SERS requires the use of metal surfaces fulfilling the Surface Plasmon Resonance condition in the region of the laser light employed for Raman excitation. This implies the use of mainly Ag, Au, and Cu having nanostructured morphology.

In practice, it is also important the absence on the surface of impurities, since the SERS technique is so sensitive that very low concentrated non-desired adsorbates can also be detected appearing spurious bands in the SERS spectra [39-40].

During the past decades, many different methods have been proposed for the preparation of metal nanostructured substrates valid for SERS involving silver colloids [41-45], silver islands [46-48], silver coated nanoparticle-based materials [49-51], polymer based substrates and electrochemically roughened electrodes.

Polymeric materials are started to be used for the preparation of SERS substrates as they are inexpensive, easy to prepare and to use. There are some applications of organic polymers on the preparation of SERS active substrates. In most of these studies, produced polymers are used as solid supports providing required surface roughness.

Kim et al. [52] used electrolyzes plating method that can be used to prepare Ag-coated polystyrene beads. Robust Ag nanostructures were reproducibly fabricated by soaking polystyrene beads in ethanolic solutions of $AgNO_3$ and butylamine.

Ag-deposited polystyrene beads were highly efficient SERS substrates, with an enhancement factor estimated using 4-aminobenzenethiol as a model adsorbate to be larger than 1.1×10^6.

Lin and Yang [53] obtained novel silver/poly(vinyl alcohol) (PVA) nanocomposite films , in which the silver nitrate, poly(g-glutamic acid) (PGA), and PVA acted as precursor, stabilizer, and polyol reducant, respectively. They found that a PGA-stabilized PVA nanocomposite film revealed the presence of well-dispersed spherical silver nanoparticles with an average diameter of 90 nm. Prepared substrate presented high SERS enhancement and the enhanced factor was estimated to be 10^6 for the detection of benzoic acid.

Hasell et al. [54] embedded nanoscopic metal structures into polycarbonate matrices. They used supercritical carbon dioxide to produce silver nanoparticles in optically transparent polycarbonate matrices allowing fine scale dispersions of particles to be produced within a prefabricated polymer component. They characterized these nanocomposites by using transmission electron microscopy and UV-vis spectroscopy. They observed that substrates gives excellent responses in SERS for both 4-aminothiophenol and rhodamine 6G target molecules.

Lu et al. [55] reported a method of fabricating nanotextured Ag surfaces using a template of self-assembled inorganic-containing block copolymer, polystyrene-*b*-polyferrocenylsilane. They observed that Ag surfaces with periodically ordered nanoscale features created by the self-organized block copolymer are capable of producing enhanced Raman signals. They used benzenethiol as a probe molecule, and observed an enhancement factor of up to 10^6. They also observed that the enhancement obtained is very uniform; Raman signal variation was less than 10 %.

After Fleishmann [33] has reported an unusually strong enhanced Raman scattering signal occurred with pyridine molecules adsorbed on roughened silver

electrodes, roughed electrodes started to be frequently used as SERS active substrates.
Recently, SERS active substrates prepared by using a combination of electrochemical triangular-wave oxidation/reduction cycles and argon plasma treatment, which roughens the substrate, increasing its SERS effect [56, 57].

Tourwe and Hubin described a roughening procedure for electrodes and they obtained desired roughness with ex-situ from a halide-free electrolyte solution, through the electrodeposition of silver in a potentiostatic double potential step [58].

Geddes et al. described two reagentless methods of silver deposition. Silver was deposited on a glass which is positioned between two silver electrodes with a constant current in pure water. Illumination of the glass between the electrodes resulted in localized silver deposition. Alternatively, silver was deposited on an indium tin oxide (ITO) cathode where a silver electrode acted as the anode [59].

Liu et al. use electrochemical oxidation-reduction cycles methods to prepare surface-enhanced Raman scattering (SERS)-active silver substrates modified with TiO_2 nanoparticles to improve the corresponding SERS performances [60].

Sauer et al. prepared SERS active silver film electrodes via electrocrystalization of silver. They observed that the electrodeposition of a sufficiently large amount of silver on silver films at high over potentials leads to excellent substrates for SERS [61].

1.3 Aim of Study

In this study, the use of N-polyethereal polypyrroles, P**I**, P**II** and P**III** polymer resins synthesized through chemical oxidation of M**I**, M**II** and M**III** respectively in preconcentration studies were investigated.

N-polyetheral polypyrroles were undoped through reduction to impart ion exchange ability to the polymer resin. Preconcentration conditions such as types of reducing agent, extraction time and pH of the medium were optimized. Then La(III), Eu(III) and Yb(III) ions were preconcentrated from aqueous medium.

Later for the preparation of SERS active substrate using P**III** (ITO-P**III**-Ag**)**, firstly, a conducting film of P**III** was obtained via constant potential electrolysis of monomer (M**III**) on ITO glass and then silver particles were embedded into the polymer. In addition to ITO-P**III**-Ag SERS substrate, another SERS active surface ITO-Ag was prepared without using P**III** polymer. Following the optimization studies, performances of the slides for SERS measurements were evaluated by using brilliant cresyl blue (BCB) and crystal violet (CV). The SERS spectra of biologic molecules, para aminobenzoic acid (PABA), nicotine and nicotinic acid were taken and Raman active modes of them were compared with the literature values.

CHAPTER 2

EXPERIMENTAL

2.1 Chemicals and Reagents

i) La (III) stock solution (1000 mg L^{-1} La): Standard solution (in dilute HNO_3) Ultra Scientific

ii) Yb (III) solution (1000 mg L^{-1} Yb): Standard solution (in dilute HNO_3) Ultra Scientific

iii) Eu (III) stock solution (1000 mg L^{-1} Eu): Standard solution (in dilute HNO_3) Ultra Scientific

iv) Li (I) solution (1000 mg L^{-1} Li): Standard solution (in dilute HNO_3) Ultra Scientific

v) Na (I) solution (100 mg L^{-1} Na): Standard solution (in dilute HNO_3) Ultra Scientific

vi) Concentrated nitric acid, 36 % (w/w), J. T. Baker,

vii) Glacial acetic acid (100 %), used for buffer solution preparation was acquired from Merck KGaA Darmstadt, Germany.

viii) 0.1 M Tetrabutylammonium hydroxide (TBAOH) solution, in diluted methanol and propanol were supplied from Merck KGaA Darmstadt, Germany

ix) Silver nitrate $AgNO_3$, has been purchased from Merck KGaA Darmstadt, Germany.

x) Tetrabutylammonium perchlorate (TBAP), **Hydrazine, Acetonitrile, (S)-Nicotine, Nicotinic Acid, Brillant Cresyl Blue (BCB), Crystal Violet (CV)** has been supplied from Aldrich.

All other reagents were of analytical-reagent grade. De-ionized water obtained from a Millipore water purification system was used in sample and standard preparations. All the glassware and plastic ware were cleaned by soaking them in 10% HNO_3 for at least 24 h and then rinsing three times with distilled water and with deionized water.
For the batch sorption studies Nüve SL 350 model shaker was used to provide efficient mixing. Resin was filtered out on a vacuum filter Advantec MFS, Inc. For filtration Whatman No 41 filter paper was used.

2.2 Instrumentation

2.2.1 Inductively Coupled Plasma Optical Emission Spectrometer (ICP-OES)

For spectroscopic determination of the REEs, an ICP-OES setup was used (Direct Reading Echelle, Leeman Labs Inc.). The instrument was operated applying an incident plasma power of 1.2 kW, with the plasma gas (Ar) coolant flow rate at 18 L/min, the auxiliary Ar flow at 0.5 L/min, and the nebulizer Ar flow set at 50 psi. The sample was transported to the nebulizer using a peristaltic pump with the pump flow rate set to 1.2 mL/min. Quantitative evaluations were based on peak height measurements. La^{3+}, Yb^{3+}, Eu^{3+}, Li^{+}, Na^{+} concentrations were determined at the following emission wavelengths: 333.749 nm for La, 328.937 nm for Yb, 381.967 nm for Eu, 588.995 nm for Na, 670.784 nm for Li.

2.2.2 Raman Spectrometer

SERS measurements were performed with Jobin Yvon LabRam confocal microscopy Raman spectrometer with a charge-coupled device (CCD) detector and a holographic notch filter. The spectrograph was equipped with a 1800-grooves/mm grating and all measurements were performed with a 200-μm entrance slit. SERS excitation was provided by 632.8-nm radiation from a He-Ne laser with a total power of 20 mW.

2.2.3 Electrochemistry

Electrochemical syntheses were performed using an IEEE 488 HEKA potentiostat/galvanostat. In electrochemical studies, indium tin oxide coated quartz glass (ITO, Delta Tech. 8–12 Ω, 0.7 cm x 5 cm) was used as working electrode, Ag wire was used as reference electrode; Pt wire was used as counter electrode.

2.3 Procedure

2.3.1 Synthesis of Monomers

Monomers which were (Figure 2.1) synthesized according to procedure described in [62], acquired from Prof. Dr. Ahmet M. Önal's Laboratory.

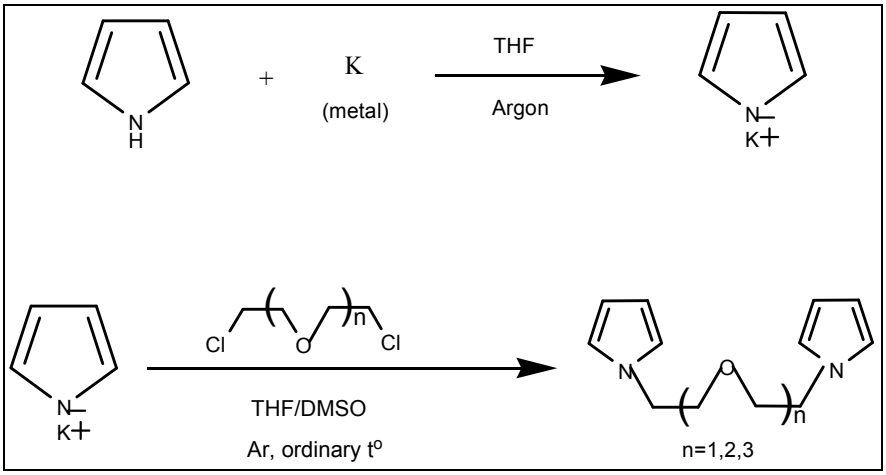

Figure 2.1. Synthesis of monomers of N-polyethereal polypyrroles.

2.3.2 Chemical Polymerization

Synthesized monomers polymerized via chemical oxidation of 1,5-bis(1,1-pyrrole)-3-oxabutane (M**I**), 1,8- bis(1,1-pyrrole)-3,6-dioxahexane (M**II**), and 1,11-bis(1,1-pyrrole)- 3,6,9-trioxaundecane (M**III**) using anhydrous $FeCl_3$ in $CHCl_3$.

2.3.3 Reduction (Undoping) of Polymer

Since as obtained polymer resins did not exhibit any affinity towards REE ions, they are reduced (undoped), prior to up-take studies, using 0.1M TBAOH solution. To assess the time required for the complete reduction of resin, 5

different batches were prepared. For each batch, 100 mg resin were suspended in 10 mL of 0.1 M TBAOH solution and equilibrated at various times (1, 2, 3, 6 and 10 days). Then, they were washed with methanol and ether, respectively. Finally, the brown powders obtained were dried under Ar atmosphere and used for the up-take and recovery measurements. To reduce resin, hydrazine was tried as a second reducing agent. 100 mg of resin were treated with 10 mL of hydrazine throughout a day. After that similar procedure as above was applied.

2.4 Optimizations for the Performance of the N-Polyethereal Polypyrroles in Preconcentration of REE

2.4.1 Up-take and Recovery Measurements

2.4.1.1 Effect of pH on Up-take Studies

The pH dependence of the metal up-take was examined by batch equilibration of the resin with buffer solutions at pH values of 2.0, 4.0, 5.0, 8.0, and 10.0. For this purpose, 50 mg of resin were suspended in 10 mL buffer solutions containing 2.0 mgL^{-1} La(III) and was equilibrated by gentle agitation. The resin was filtered out and the supernatant solution was analyzed for the metals using ICP-OES technique.

2.4.1.2 Effect of Batch Time on Up-take Study

The metal binding parameters for the resin were appraised using standard aqueous solutions. The batch procedure was accomplished by equilibrating 50 mg of the polymer resin with two different concentrations (3.0 and 0.40 mgL^{-1}) of the metals (La(III), Yb (III), Eu(III)) solutions. 3.0 mgL^{-1} and 0.40 mgL^{-1} lanthanides solutions were shaken for 5 h and 6 h respectively, and then filtered. The supernatant was separated from the resin and monitored for the metal concentrations by ICP-OES for up-take study.

2.4.1.3 Recovery Measurements of REEs

For the recovery of adsorbed metals, different concentrations of HNO_3 and HCl were tried. After the adsorption of 2.0 mgL^{-1} of La on 0.05 M of P**III**, the resin was filtered and separated from solutions and shaken up 0.5, 1, 2, 3 M of HNO_3 and HCl for 1 h and supernatants were monitored for the metal concentrations by ICP-OES for recovery studies.

2.4.1.4 The Sorption Capacity of PIII

For investigation of sorbent capacity, 10 mL of 10.0 mgL^{-1} La solution was equilibrated with 50 mg P**III** resin for 2 h. The adsorbed La (III) ions were stripped from the resin with 2 M HNO_3 and concentrations determined by ICP-OES.

2.5 Preparation of ITO-PIII-Ag SERS Active Substrate

2.5.1 Electrochemical Polymerization

Electrochemical polymerizations were performed in three-electrode cell (Figure 2.2). Ag-wire, Pt-wire and ITO glass electrodes were used as reference electrode, counter electrode and working electrode respectively. P**III** were grown applying oxidation potential of related monomer (1.2 V vs. Ag-wire) in 0.05 M TBAP solution containing 20 μl of monomer. 5, 15, 20, 60 mC/cm^2 on ITO working electrode and the bright black film formed on working electrode with different thicknesses at the end of electrolysis.

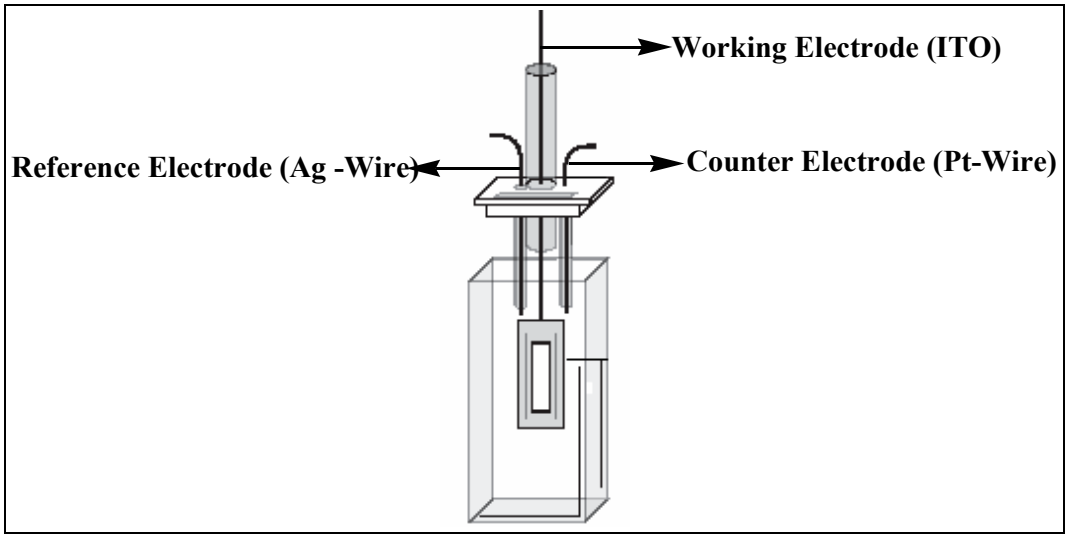

Figure 2.2. Shematic diagram of classical three-electrode cell.

2.5.2 Deposition of Silver Nanoparticles on ITO-PIII-Ag Substrate

Ag(I) ion was reduced to metallic silver on P**III** coated ITO via electrolysis. 5 mL of 0.05 M $AgNO_3$ solution was prepared in acetonitrile, containing 0.05 M TBAP. Ag(I) was reduced to metallic silver by applying -0.5 V,-0.7 V,-0.8 V vs. Ag-wire (reduction potential of silver). Deposition processes were carried out at various charge densities for the reduction of silver: 20; 40; 80; 100; 120 mC/ cm^2.

2.6 Preparation of ITO-Ag Substrate

In this substrate Ag(I) ion was reduced to metallic silver directly on ITO glass via electrolysis. 5mL of 0.05 M $AgNO_3$ solution was prepared in acetonitrile, containing 0.05 M TBAP, Ag(I) was reduced to metallic silver by applying -0.7 V vs. Ag-wire (reduction potential of silver) and deposition process were carried out at various charge densities for the reduction of silver: 5; 15; 20; 60 mC/ cm^2.

2.7 Evaluation of the Performance of SERS Active Substrates

The performance of SERS active substrates are evaluated by using solutions of Brillant Cresyl Blue BCB, Para aminobenzoic acid PABA, Crystal Violet CV, (S)-nicotine and nicotinic acid at different concentrations.

CHAPTER 3

RESULTS AND DISCUSSION

3.1 The Performance of N-Polyethereal Polypyrroles for the Preconcentration of REEs

In this study, firstly N-polyethereal polypyrroles were undoped using two reducing agents to impart an ion exchange ability to the polymer resin. Preconcentration studies were carried out for La(III), Eu(III) and Yb(III) from aqueous medium.

3.1.1 Comparison of (PI, PII, PIII) Resins for the Preconcentration Studies

For the selection of effective sorbent for REE ions below experiments were done. One cage, two cages and three cages of N-polyethereal polypyrrole (P**I**, P**II**, P**III**) resins were examined for the preconcentration studies of REE ions. For this purpose the undoped polymer resins P**I**, P**II**, P**III** were tried in the extraction of REE ions from aqueous medium and the results are tabulated in Table 3.1. As seen from Table 3.1, the percentage recovery values for P**I** and P**II** are almost eight times lower than that of P**III**.

Table 3.1. Recoveries obtained with N-Polyethereal Polypyrrole Resins (P**I**, P**II** and P**III)** for 0.4 mg L^{-1} La(III).

Type of Resin	Initial volume(mL)	Final volume(mL)	Enrichment Factor	% Recovery
P**I**	40	8	5	14
P**II**	40	8	5	12
P**III**	40	8	5	**98**

This might indicate the presence of cavities with different sizes on the polymer backbone (Figure 3.1) which is contradictory to the polymer structure with uniform cavity size P**I**, P**II** and P**III** suggested by Simonet et al. [2].

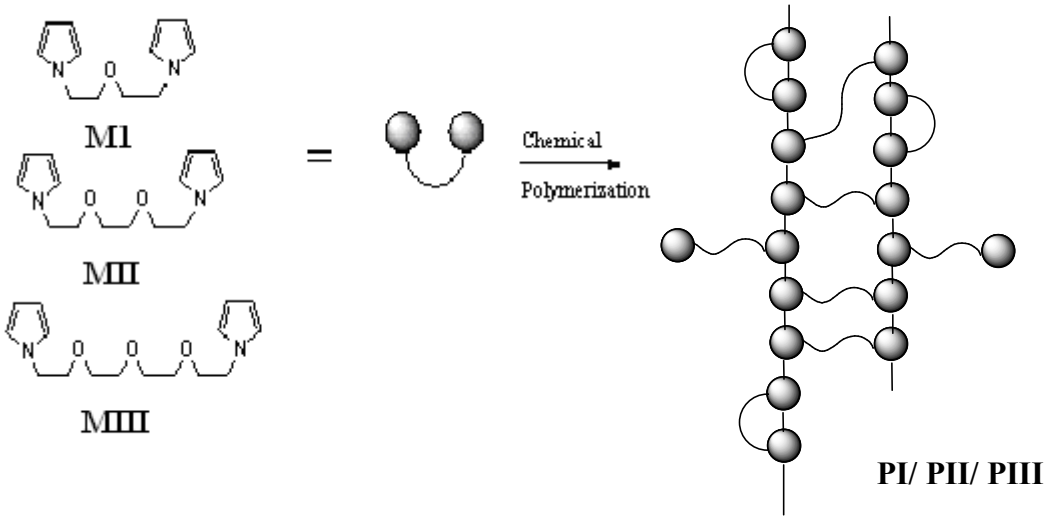

Figure 3.1. Polymerization of three different N-polyethereal pyrrole monomers (M**I**, M**II** and M**III**).

3.1.2 Reduction of PIII Resin

It is necessary to reduce the polymer resin in order to remove part of the anions arising from the electrolyte. This reduction can be carried out chemically or

electrochemically. For this part, P**III** was reduced via chemical method, as follows.

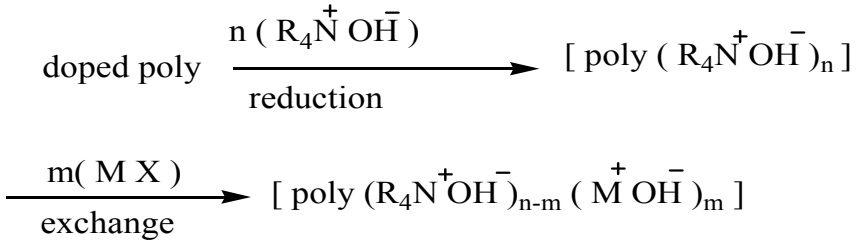

Reduced polymers in the neutral form can behave as ion exchange resins and particularly have the property of extracting metal ions present in aqueous or organic solutions, provided that the resins are treated beforehand with ammonium salts such as tetraalkylammonium hydroxide, which makes the change between ammonium ions and metal ions.

3.1.2.1 Selection of Reducing Agent

Initially TBAOH was tried as a reducing agent. Because the reduction with TBAOH takes a long time, alternative reducing agent, hydrazine, was also tried in this study. Results are discussed in Table 3.3.

Table 3.2. Up-take and recovery values of 2.0 mgL^{-1} La with 50 mg resin treated different types of reducing agent.

Type of Reducing Agent	Time of Reduction	% up-take	% Recovery	Regeneration
Hydrazine	1 day	98	88	_
TBAOH	10 days	100	98	+

As can be seen from Table 3.3, although using TBAOH as a reducing agent reduction taking a long time however, it was selected as a reducing agent because, hydrazine causes structure deformation of P**III**. Therefore P**III** treated with hydrazine did not respond cations at the second usage. Since the regeneration is an important determinant for the usage of ion exchange resins further experiments by using TBAOH as reducing agent.

3.1.2.2 Time of Reduction of PIII

In order to find the optimum time for the reduction, conducting polymer P**III** were undoped (reduced) at various times (1, 2, 3, 6 and 10 days) using TBAOH. The capabilities of these 5 different P**III** resins for the extraction of La(III) from aqueous solutions were then examined Figure 3.2.

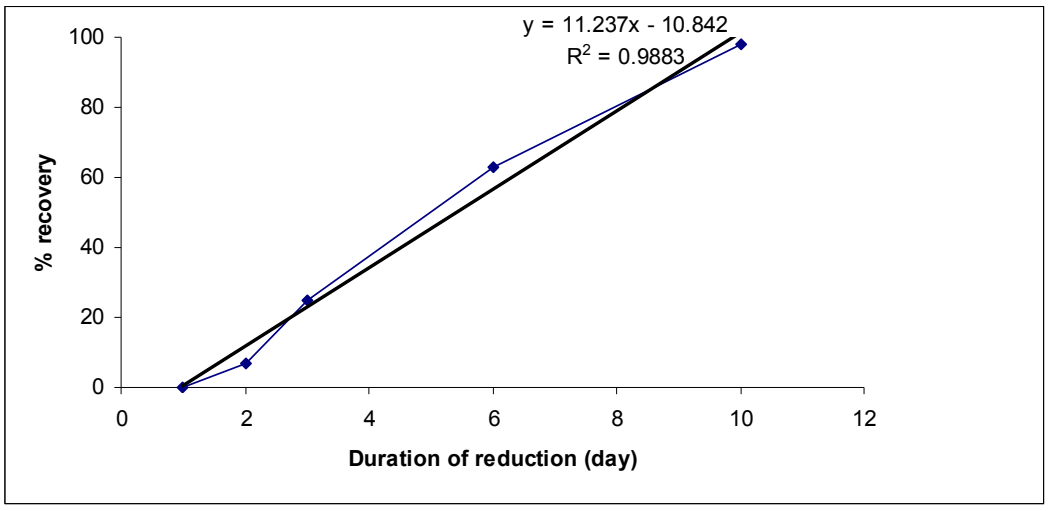

Figure 3.2. Variation of recovery with duration for the extraction of 0.40 mgL^{-1} La(III). La(III) solution by P**III** resin depending on the span of undoping (reduction) process of polymer P**III** with 0.1 M TBAOH.

As can be seen from Figure 3.2, the 100 % recovery of La(III) ions was obtained with the resin reduced at 10 days with 0.1 M TBAOH. Therefore, in the chemical

preparation of resins for metal cation extraction studies duration of resin reduction was chosen as 10 days.

3.1.3 Optimizations for the Performance of the PIII in Preconcentration of REEs

3.1.3.1 Effect of pH on Up-take Study

It is known that the up-take efficiency of the any ion exchange resin depends on pH of the solution. In order to find optimum pH at which P**III** polymer resin is effective to hold REE ions, buffer solutions at different PH's were prepared. (Section 2.4.1.1). The percent recovery- pH diagram is given in Figure 3.3.

Batch equilibration studies of the partition of lanthanum between P**III** resin and solutions having various acidities showed that this metal was taken up almost %100 by the P**III** resin over a pH range of 5-10 (Figure 3.3). And further experiments were performed at pH 5. As expected, the percent recovery values changes similarly for the extraction of Yb(III) and Eu(III) with P**III** resin depending on the pH.

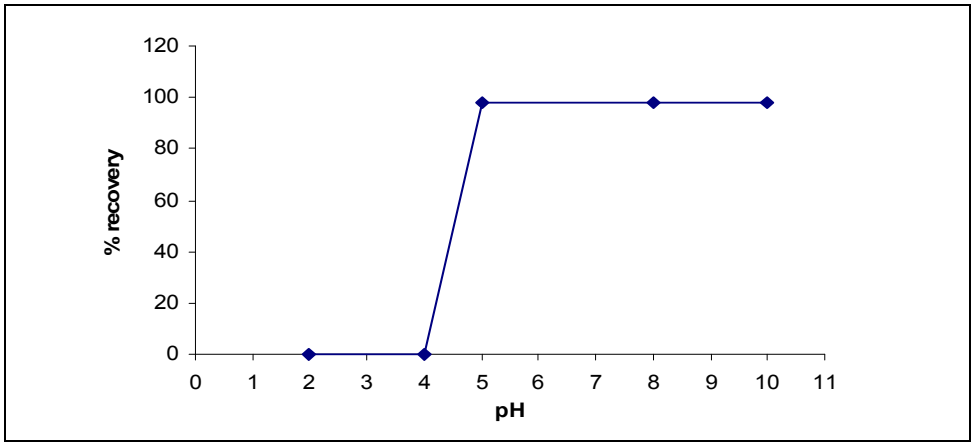

Figure 3.3. Batch equilibration of 2 mgL^{-1} La(III) with 50 mg P**III** resin as a function of pH. Equilibration time was 2 h.

3.1.3.2 Effect of Batch Time to Up-take Studies

One more study was optimizing the rate of the take up of the P**III** polymer resin for REE ions. To optimize batch equilibration time 3 mgL^{-1} and 0.4 mgL^{-1} solutions of La(III), Yb (III), Eu(III) with 0.05 g resin were carried out up to 6 h for up-take studies. The rate of the equilibration of P**III** resin with REE ions was found to be rather slow. 4 h of shaking was needed for batch type extraction of 3 mgL^{-1} metal ion concentration. The adsorption rate becomes even slower (6 h) at a concentration of 0.4 mgL^{-1} (Figure 3.4 and 3.5). However, aqueous solutions of these ions are stable and they do not undergo any appreciable change during lengthy periods of shaking. Therefore, the long span of equilibration does not affect percent recoveries.

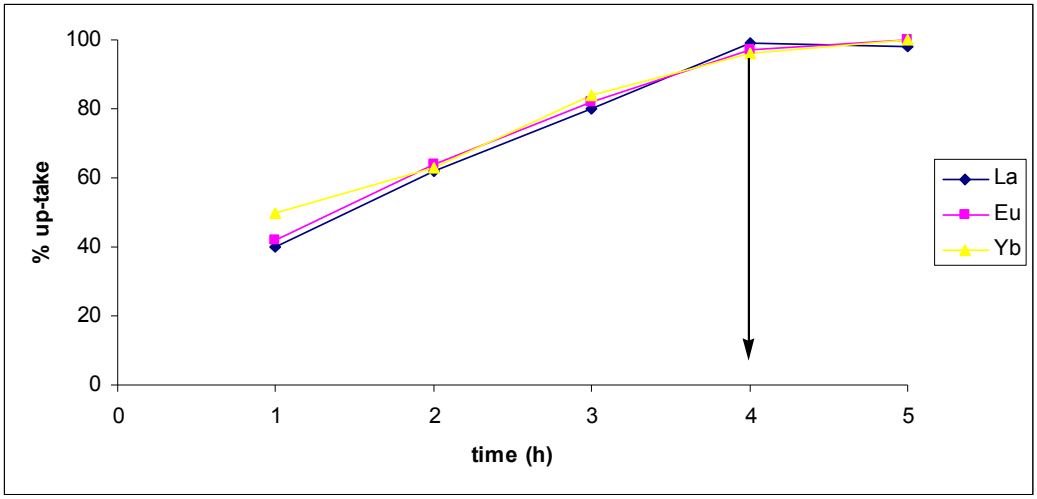

Figure 3.4. Up-take percentage of as a function of time,10 mL solution containing 3.0 mgL^{-1} La, Eu, Yb ; 50 mg P**III**.

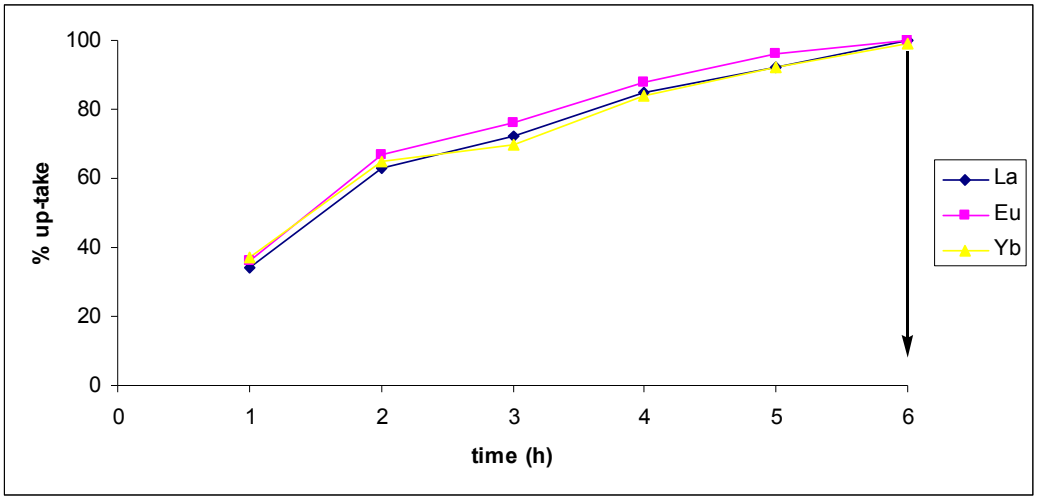

Figure 3.5. Up-take percentage of as a function of time, 10 mL solution containing 0.40 mgL^{-1} La, Eu, Yb ; 50 mg P**III**.

3.1.3.3 Recovery of REEs from PIII Resin

After collection of La(III) on P**III** resin (up-take), the recovery of La(III) from the resin was studied. Potentially suitable eluting acids like HCl and HNO_3 were tried to recover the adsorbed REE ions. Similar recoveries were obtained with different HNO_3 concentrations applied and 2 M was decided to be used for recovery from P**III** polymer resin. Recovery yields using 2 M HNO_3 were higher than 95 % as seen in Figure 3.6. Therefore, recovery studies were performed using 2 M HNO_3

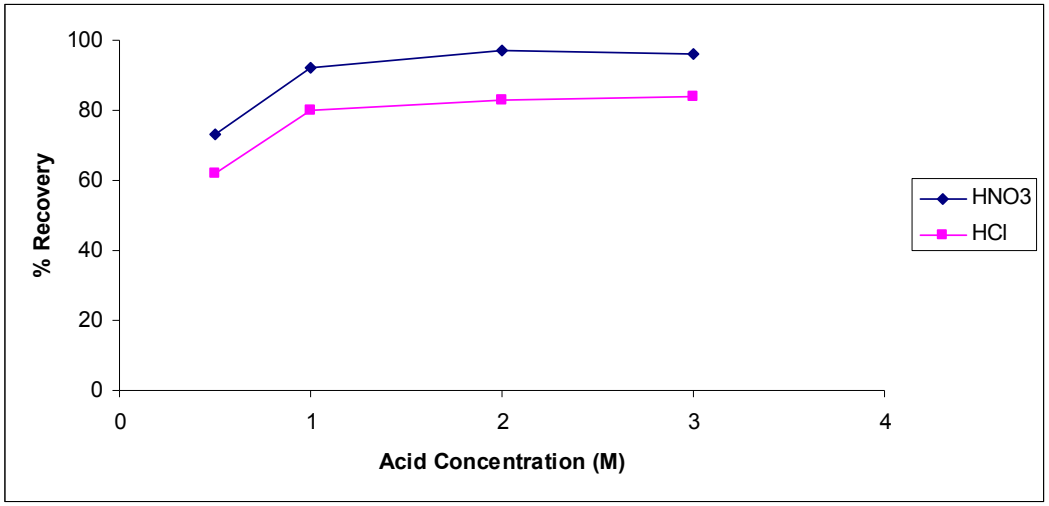

Figure 3.6. Effect of acids concentrations on recovery % Recovered metal was 2 mg L^{-1} La(III). Equilibration time was 1h.

3.1.3.4 Capacity of Sorbent

The capacity of the sorbent is an important factor that determines for predicting the amount of sorbent required to quantitatively remove a specific amount of metal ion from the solution so the sorption capacity of the P**III** resin was measured and it was found as 1.340 mg of La(III) / g P**III** resin.

3.1.4 Preconcentration of REEs

As it was mentioned in the previous section three of REE ions were selected for the preconcentration studies. La(III) representing the light REE's, Eu(III) was selected for the middle REE's and Yb(III) for the heavy REE's were selected as representative.

The extraction efficiencies of P**III** resin for La(III), Yb(III), Eu(III) were examined for a concentration range of 3.0-0.4 mg L^{-1}. As shown in Table 3.4, high recoveries obtained for investigated concentrations indicated that, successful pre-concentrations of REEs from aqueous solutions were possible with P**III** resin.

For La(III) ions lower concentrations were also investigated. Recovery values of 98 % and 75.5 % were obtained for 0.1 and 0.04 mgL^{-1} concentrations of La(III) ions, respectively.

Table 3.3. Percent Recoveries obtained with P**III** resin at various concentrations of La(III), Yb(III), Eu(III) ions from aqueous solutions.

Cations	Spiked concentration (mg /l)	Initial Volume (mL)	Final Volume (mL)	Enrichment factor	% Up-take	% Recovery
La(III)	3	10	10	1	99.1±0.8	91.4±4.8
	0.4	40	8	5	100±0.1	98 ±1.0
	0.1	40	8	5	100±0.1	98±3.0
	0.04	100	5	50	<DL	75.5±2.0
Eu(III)	3	10	10	1	99.9±0.2	90.7±1.4
	0.4	40	8	5	100±0.1	90.5±1.2
Yb(III)	3	10	10	1	99.9±0.1	90.7±3.1
	0.4	40	8	5	100±0.1	87.3±4.0

Recovery and Up-take results are the average of three individual measurements.

3.1.5 Regeneration of PIII Resin

The efficiency of ion exchange resins is also evaluated by regeneration times. In order to assess the extent to which the performance of the P**III** resin deteriorates following elution with 2 M HNO_3, the same resin was employed for five consecutive pre-concentration stripping cycles for La(III).

As it was mentioned before P**III** polymer resins activity depends on it is in reduced form. After it was used, P**III** polymer resin interacted with oxygen in air and thus it was oxidized at each use. Therefore after each use the resin was

reduced with TBAOH to regenerate its sorption capacity. Reduction procedure was given in previous chapter.

As can be seen from the Table 3.5 excluding 4th usage the percent take-up values are all hundred. Although the percent recovery values show slight decrease at 4th and 5th usages of the P**III** resin, they are still at acceptable levels for a pre-concentration work (≥90 %).

Table 3.4. Recoveries obtained for the extraction of 0.4 mgL^{-1} La(III) ions with re-used P**III** resins.

Number of Usage	% Up-take	% Recovery
1st	100	96.0
2nd	100	96.0
3rd	100	97.3
4th	98.5	91.4
5th	100	90.0

3.2 ITO-PIII-Ag SERS Substrate

Electrochemistry provides a means by which many metals and alloys can be deposited onto a conductive surface from an electrolyte. In the preparation of SERS active substrate using P**III** (ITO-P**III**-Ag**)**, firstly conducting film of P**III** was obtained via constant potential electrolysis of monomer M**III** on ITO electrode and then silver particles were deposited onto the polymer. The electrochemical polymerization of the monomer M**III** was done according to Cihaner's procedure [1]. Hence, optimization studies were focused on to the introduction of silver metal into the polymer matrix, in other words electrolysis of silver on P**III** coated ITO electrode .

In addition to ITO-PIII-Ag SERS substrate, another SERS active surface was prepared without P**III** polymer. Hence, bare ITO plates were electroplated with silver directly and used as SERS substrates. Following the optimization studies, performances of the slides for SERS measurements were evaluated by using brilliant cresyl blue (BCB) and crystal violet (CV). The SERS spectra of biologic molecules, para amino benzoic acid (PABA), nicotine and nicotinic acid were taken and Raman active modes of them were compared with the literature values.

3.2.1 Optimization Studies of ITO-PIII-Ag Substrate

The magnitude of the SERS effect depends critically on the size, shape and spacing of the metal nanostructures [48, 63]. An optimal size for the roughness features between 10 and 100 nm, depending on the experimental conditions, has been frequently reported [64, 65].

We were hoping to obtain tailor made distributions of SERS active silver particles on the polymer coated ITO substrates. The morphology (cluster density, mean particle size and degree of size dispersion of silver and therefore the SERS enhancement factor) of the resulting surface depends strongly on the electrochemical parameters applied during the deposition process such as electrolyte composition, applied potential and charge density. Therefore, silver nitrate concentration; reduction potential of silver and total charge per total electrode area (charge density) for the deposition of polymer and silver were optimized. Each parameter was changed one at a time and the SERS performances of the prepared slides were evaluated by using BCB as a model compound.

3.2.1.1 Electrochemical Polymerization of MIII

ITO coated glass slides were used as working electrode. It is known that ITO is stable in the potential region of +1 V to -1.2 V but at more negative potentials reduction of ITO occurs [65]. Electrochemical polymerization conditions of M**III** and PIII had been studied previously [1]. The electrochemical data acquired are

tabulated in Table3.6. In this study M**III** was polymerized at 1.2 V vs. Ag-wire in 0.05 M TBAP dissolved in acetonitrile. A bright black film coated on the surface of ITO glass at the end of the electrolysis. The electroactive polymer was well adhered to the ITO coated glass working electrode.

Table 3.5. Electrochemical data for PIII.

Monomer	**Polymer**	
MIII	**PIII**	
E_{pa}(V)	E_{pa}(V)	E_{pc}(V)
1.15	0.7	0.52

3.2.1.2 Silver Nitrate Concentration

The concentration of $AgNO_3$ in acetonitrile was varied as 0.005, 0.01, 0.02, 0.05 M The intensity of the SERS spectrum of 10^{-6} M BCB was compared for the substrates prepared by indicated concentrations of $AgNO_3$. The highest intensity was acquired when 0.05 M $AgNO_3$ was used.

3.2.1.3 Reduction Potential of Silver

The effect of the reduction potential of silver on the SERS enhancement was examined for three different potentials (-0.5 V, -0.7 V and -0.8 V). Although there were not significant differences among them, the substrate prepared at -0.7 V reduction potential gave slightly more intense SERS peak for 10^{-6} M BCB. Therefore, all experiments reported here after were carried out using 0.050 M $AgNO_3$ and -0.7 V reduction potential for silver.

3.2.1.4 Total Charge Per Total Area of the Substrate

In this section, we tried to optimize charge density both for polymer and silver deposition for the same substrate. First of all the charge density for polymer deposition was changed as 5, 15, 20 and 60 mC/cm^2. Slides coated with various amount of polymer (or with various thickness of polymer) were doped with silver. During silver deposition the charge density was kept constant at 80 mC/cm^2. Thus, prepared substrates were tested for their surface enhanced Raman activity using 10^{-6} M BCB. Conditions used for the substrate preparation and signal intensities of BCB acquired with these substrates are summarized in Table 3.6.

Table 3.6. Conditions used for the SERS substrate preparation with various polymer thickness and signal intensities of 10^{-6} M BCB acquired with these substrates.

Ag (M)	**TBAP (M)**	**MIII (V)**	**Polymer mC/cm^2**	**Ag(I) (V)**	**Ag(I) mC/cm^2**	**10^{-6} M BCB Raman Intensity**
0.05	0.05	1.2	5	-0.7	80	2500
0.05	0.05	1.2	15	-0.7	80	**11000**
0.05	0.05	1.2	20	-0.7	80	**10000**
0.05	0.05	1.2	60	-0.7	80	5000

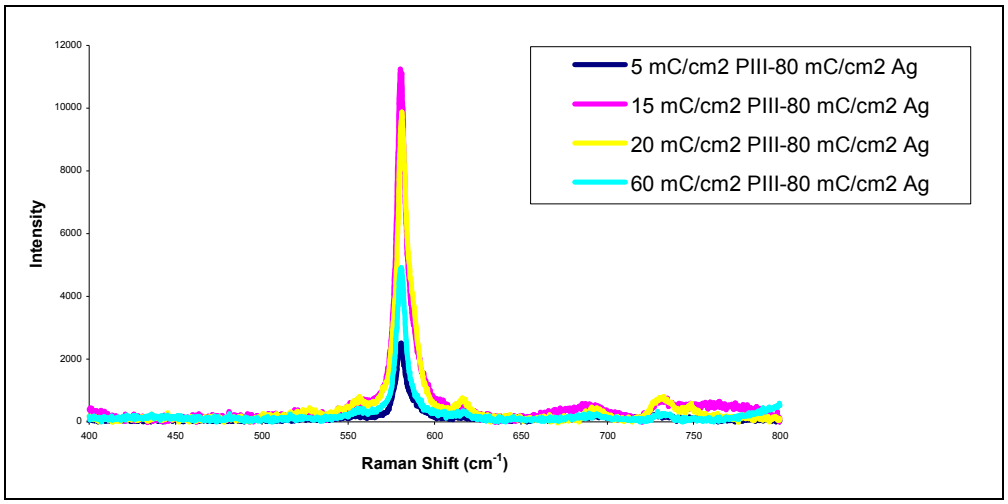

Figure 3.7. SERS spectra of 10^{-6} M BCB obtained by ITO-P**III**-Ag substrates prepared at conditions stated in Table 3.6. Various charge densities (5, 15, 20, 60 mC/cm^2) were used during polymer coatings.

As can be seen from Table 3.6 and Figure 3.7, comparatively high BCB signals were obtained with the substrates prepared when a charge density of 15 mC/cm^2 and 20 mC/cm^2 were used during polymer deposition. Since the homogeneity of the substrate was better in the second case, although the BCB signal intensity is slightly small, 20 mC/cm^2 was chosen as the optimum charge for the deposition of the polymer. Afterwards ITO glasses were coated with polymer at a charge of 20 mC/cm^2 and doping processes were carried out at various charge densities for the reduction of silver: 20, 40, 80, 100 and 120 mC/cm^2. Substrates doped with various amount of silver were tested for their surface enhanced Raman activity using 10^{-6} M BCB. Conditions used for the substrate preparation and signal intensities of BCB acquired with these substrates are given in Table 3.7 and Figure 3.8.

Table 3.7. Conditions used for the preparation of substrates doped with various amount of silver and signal intensities of 10^{-6} M BCB acquired with these substrates are given.

Ag(I) (M)	**TBAP (M)**	**MIII (V)**	**MIII mC/cm^2**	**Ag(I) (V)**	**Ag(I) mC/cm^2**	**10^{-6} M BCB Raman Intensity**	**SEM Images**
0.05	0.05	1.2	20	-0.7	20	6000	
0.05	0.05	1.2	20	-0.7	40	**13000**	Surface 1
0.05	0.05	1.2	20	-0.7	80	**19000**	Surface 2
0.05	0.05	1.2	20	-0.7	100	11000	
0.05	0.05	1.2	20	-0.7	120	8000	

As can be seen from the Table 3.7 and corresponding SERS spectra exhibited on Figure 3.8, the highest SERS intensity for BCB was obtained when the charge density was 80 mC/cm^2 during silver doping.

According to the experiments carried out, it was concluded that surfaces exhibiting the highest SERS enhancement factor were prepared by using $AgNO_3$ concentration of 0.05 M in acetonitrile, a potential of -0.7 V and by allowing 20 mC/cm^2 and 80 mC/cm^2 charge densities for polymer coating and for the reduction of silver respectively.

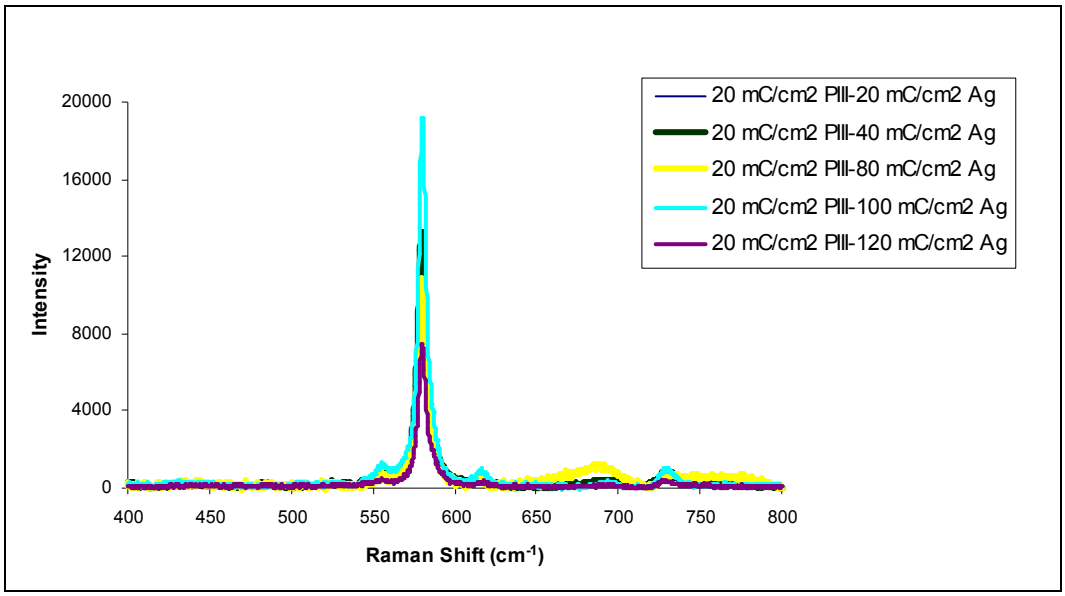

Figure 3.8. SERS spectra of 10^{-6} M BCB obtained by ITO-P**III**-Ag substrates prepared at conditions stated in Table 3.7. Various charge densities (20, 40, 80, 100 and 120 mC/cm^2) were used during reduction of silver on P**III** coated ITO slides.

To test the spatial uniformity in signal intensity of ITO-P**III**-Ag substrates mentioned in Tables 3.6 and 3.7, SERS spectra of 10^{-6} M BCB were acquired using as many different locations as possible on these substrates. The signal intensities were varying considerably on changing the location. In most of the sites of these surfaces SERS enhancement factor was almost zero. As shown in Figure 3.9, only at a few distinct locations of the substrates SERS signals of BCB were obtained. These Raman active spots are called as 'hot points'. The intensity values of BCB tabulated in Tables 3.6 and 3.7 are the highest intensities selected among these hot points of each substrate. This behavior could be rationalized based on the different morphologies of the silver particles formed under different conditions.

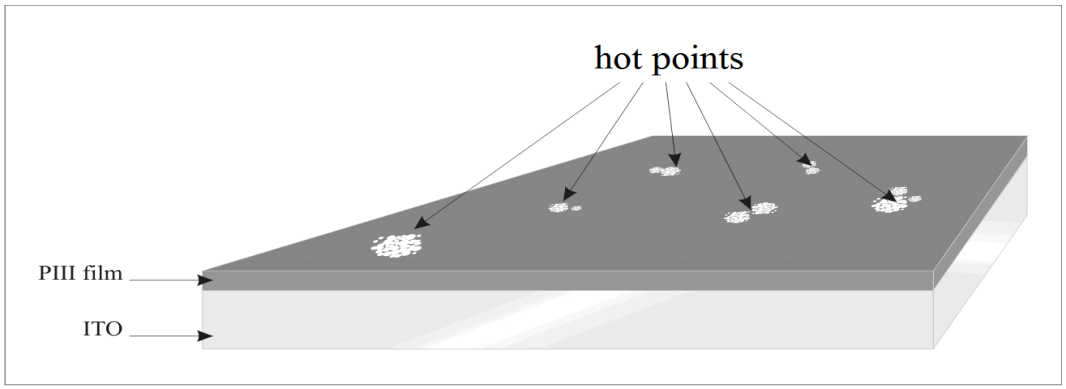

Figure 3.9. Schematic representation of the Raman active spots (hot points) on ITO-P**III**-Ag substrate.

The surface densities as well as average diameter and variation of the size distributions were investigated by taking the SEM images of two substrates that provided high BCB signals at their hot points (Table 3.7) to evaluate the influence of the surface morphology. The total charge for polymer coating was kept at 20 mC/cm^2, whereas the charge density of silver deposition was taken as 40 mC/cm^2 (Surface 1) and 80 mC/cm^2 (Surface 2). Figure 3.10a shows a scanning electron micrograph (SEM) image of the silver flakes on surface1. As can be seen from the Figure 3.10a the whole surface is covered but they are not densely located and there is a local variation in their distribution. The flake like structures and the dark spaces around them were inspected at higher magnification (Figure 3.10b and c). The lichen-like shape shows that they are clusters of Ag crystallites (Figure 3.10b) with an average size of 30 μm. As can be seen from the Figure 3.10c, there are silver particles around 230 nm size which are unevenly distributed around the flakes. Both the size of the particles and the flakes are much larger than suitable size range for SERS. The lack of SERS enhancement in most of the regions of this substrate is probably related with the size of the silver particles and the clusters. Although quite rare, there are some tiny particles among the silver particles and most likely hot points are matching up with these regions.

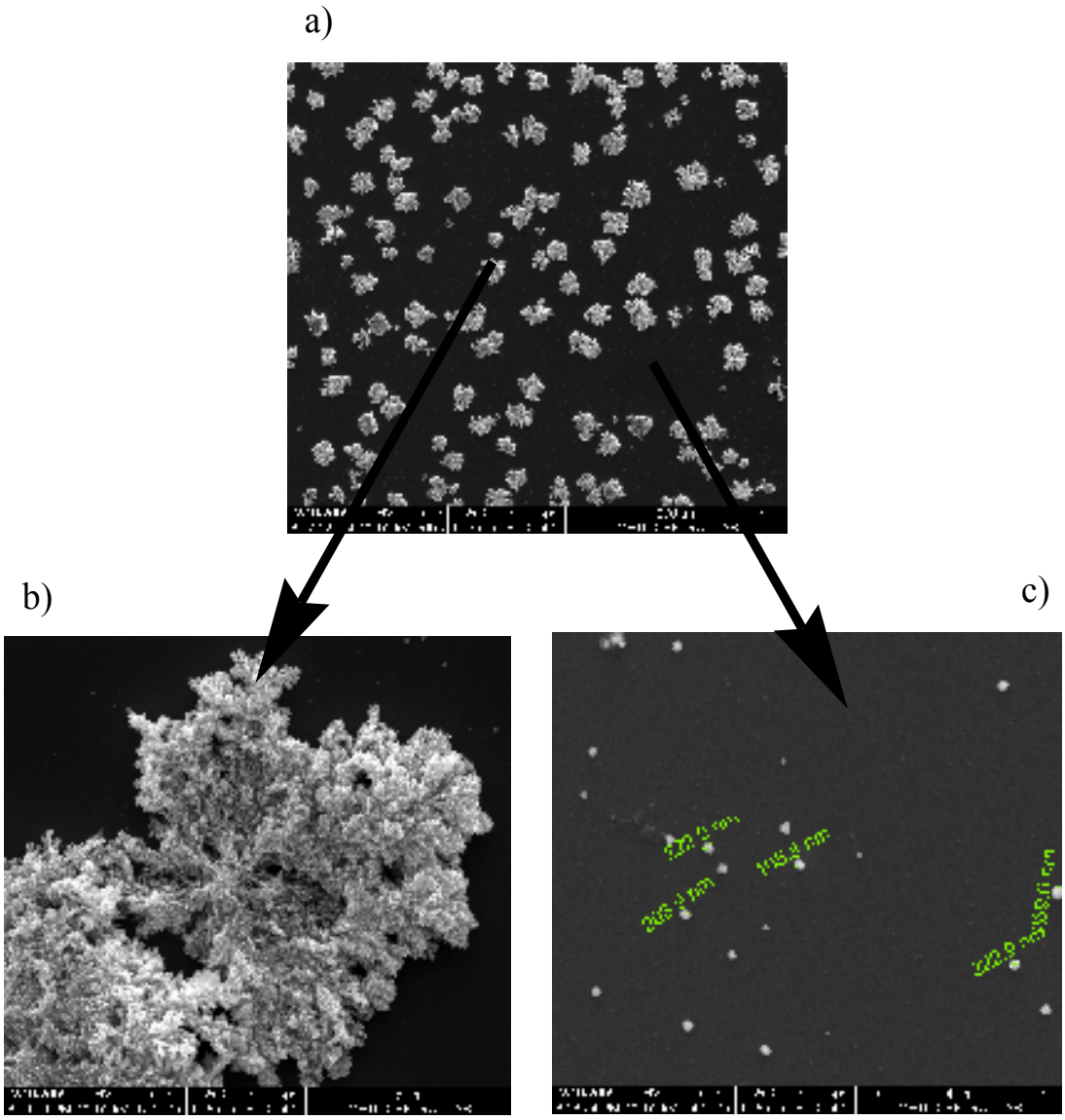

Figure 3.10. FE-SEM images of Surface 1 a) image of the silver flakes at 500x magnification b) image of the flake structures at 12000x magnification c) image of dark spaces seen in part (a) at 24000x magnification.

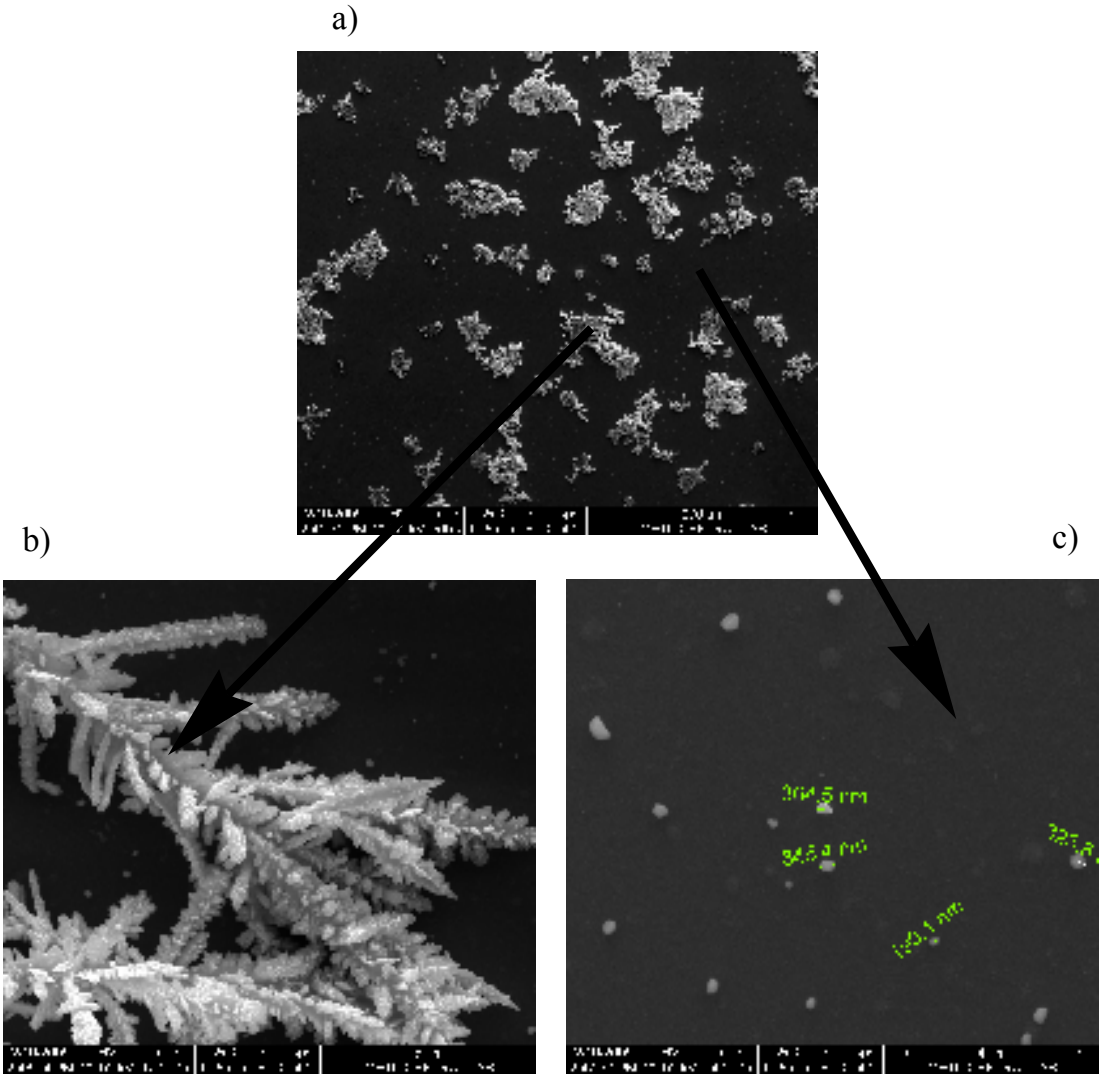

Figure 3.11. FE-SEM images of Surface 2 a) image of the silver flakes at 500x magnification b) image of the flake structures at 12000x magnification c) image of dark spaces at 24000x magnification.

Figure 3.11 depicts the SEM images of Surface 2 at different magnifications. As seen from Figure 3.11a when the total charge per cm^2 is increased from 40 to 80 mC/cm^2 the size homogeneity of the flakes is totally disturbed. This seems to be the result of a destabilization of the clusters because of overlapping diffusion zones [66-68]. If diffusion zones of larger clusters overlap with a diffusion zone of a small particle, the larger cluster draws an increased disproportionate fraction

of the electrolyte at the expense of the growth of the smaller particle. Thus, the lack of electrolyte in the solution around the smaller particle can turn a formerly stable cluster into an unstable state and the cluster dissolves [66-68]. Furthermore, lichen-type cluster shapes turn into small three like growths of silver deposition with ramifying branches and fine leafy structures (Figure 3.11b) and silver particles become larger (Figure 3.11c). Roughly speaking, based on the size measurement that we have done on SEM micrographs, we can say that two-fold increase in charge density during silver reduction increased the sizes of the clusters and particles almost twice. This fact indicates that crystal growth dominates over nucleation i.e. the electrocrystallization process favours the reduction of silver on already present nuclei instead of forming new ones. Therefore, as we have stated before the presence of few hot points all over the surface of the substrates can be associated to the presence of some small particles difficult to see with field emission scanning electron microscopy (FE-SEM) technique.

3.3 ITO-Ag SERS Substrate

In this section, the optimization of the parameter for the direct electrodeposition of silver on ITO coated glass surface; investigation of the SERS activity of the surfaces and the surface characterization of the prepared substrates via FE-SEM measurements will be presented.

3.3.1 Optimization Studies of ITO-Ag Substrate

$AgNO_3$ concentration (0.05 M), reduction potential of silver (-0.7 V vs. Ag-wire) and ITO glasses and have been utilized in the preparation of ITO-PIII-Ag substrate were used in the preparation of ITO-Ag Substrate. The polymer coating step was excluded and various surfaces were produced by altering the current density during electrodeposition of silver. The SERS performances of each surface were examined by acquiring the SERS spectrum of 10^{-6} M BCB. Electrochemical parameters used for the preparation of ITO-Ag SERS substrates

loaded up with various amount of silver and signal intensities of 10^{-6} M BCB acquired with these substrates are given in Table 3.8.

Table 3.8. Electrochemical parameters used for the preparation of ITO-Ag SERS substrates loaded up with various amounts of silver and signal intensities of 10^{-6} M BCB acquired with these substrates.

Ag(I) (M)	**TBAP (M)**	**Ag(I) (V)**	**Ag(I) mC/cm^2**	**10^{-6} M BCB Raman Intensity**
0.05	0.05	-0.7	5	8600
0.05	0.05	-0.7	10	≥64000
0.05	0.05	-0.7	20	33000
0.05	0.05	-0.7	70	17000

The signal intensities given in Table 3.8 are comparable or better than the ones obtained with ITO-P**III**-Ag substrates at their hot points. The highest signal intensity for 10^{-6} M BCB was obtained on the ITO surface coated with silver at 10 mC/cm^2 charge density. The uniformity of the surfaces in terms of SERS activity were inspected as explained in section 3.2.1.4. Besides their high SERS enhancement properties, the surface homogeneity of the ITO-Ag substrates were better than that of ITO-P**III**-Ag substrates. Figure 3.12 shows the SERS spectra of 10^{-6} M BCB taken at different locations of ITO-Ag substrate prepared at a charge density of 5 mC/cm^2 (Table 3.8). The variation in signal intensity between the spots is around 30.0 %. (Figure 3.13). Although not shown, the other ITO-Ag substrate surfaces illustrate similar variation in their SERS enhancements.

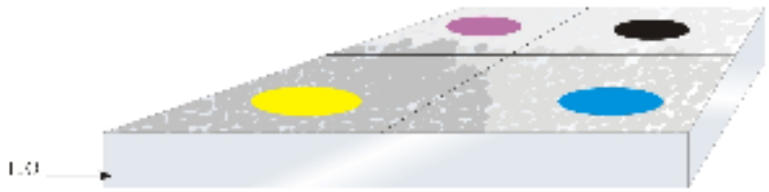

Figure 3.12. Sampling locations of 10^{-6} M BCB on ITO-Ag substrate prepared at charge density of 5 mC/cm^2.

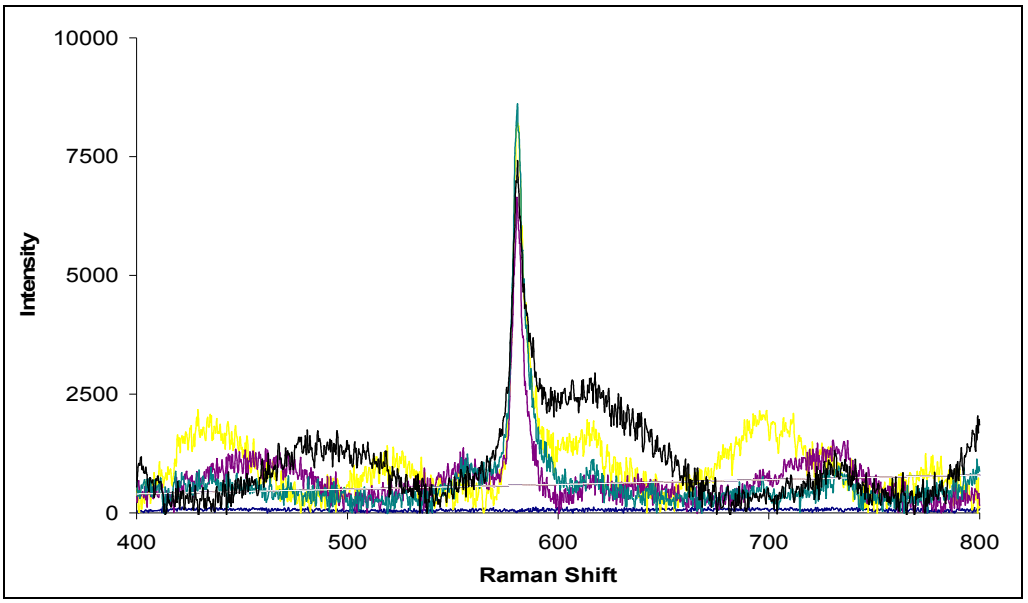

Figure 3.13. SERS spectra of 10^{-6}M BCB taken at different locations of ITO-Ag substrate (Figure 3.12) prepared at charge density of 5 mC /cm^2. The intensity range is 8600-6200.

Figure 3.14 shows FE-SEM images of ITO-Ag substrates taken after the deposition of silver at various charge densities. The gray stains on the surface could be due to electrochemical reduction of ITO. Compared to ITO-P**III**-Ag substrate a uniform distribution both in terms of size and particle density

observed. The particle diameters increase as expected with increasing growth time. This fact can easily be visualized at larger magnification of the same images (Figure 3.15). The shape of the particles indicate that nucleation starts on the ITO surface, and then these spherical particles provide nucleation sites for the formation of new spheres that are adhered to the previous ones and further increase in deposition lead to the formation of a cauliflower like clusters. As we have observed in the preparation of ITO-P**III**-Ag substrates, again crystal growth dominates over nucleation with the effect that larger crystals are formed instead of densely formed small crystals. Therefore, the establishment of the first nucleation and the controlled growth afterwards are very critical in the preparation of SERS substrates. However, even though the electrodeposition conditions are adjusted properly irreproducibility of the SERS intensity may arise related to the surface morphology of the ITO glass. It is impossible to obtain exactly the same surface for each experiment. Therefore, it can be expected that, when performing comparable experiments, the random distribution of nuclei on the surface will never be identical. Consequently, the overlap between the depletion layers will also be different, resulting in a different particle size distribution, which is responsible for the limited reproducibility of the SERS intensities.

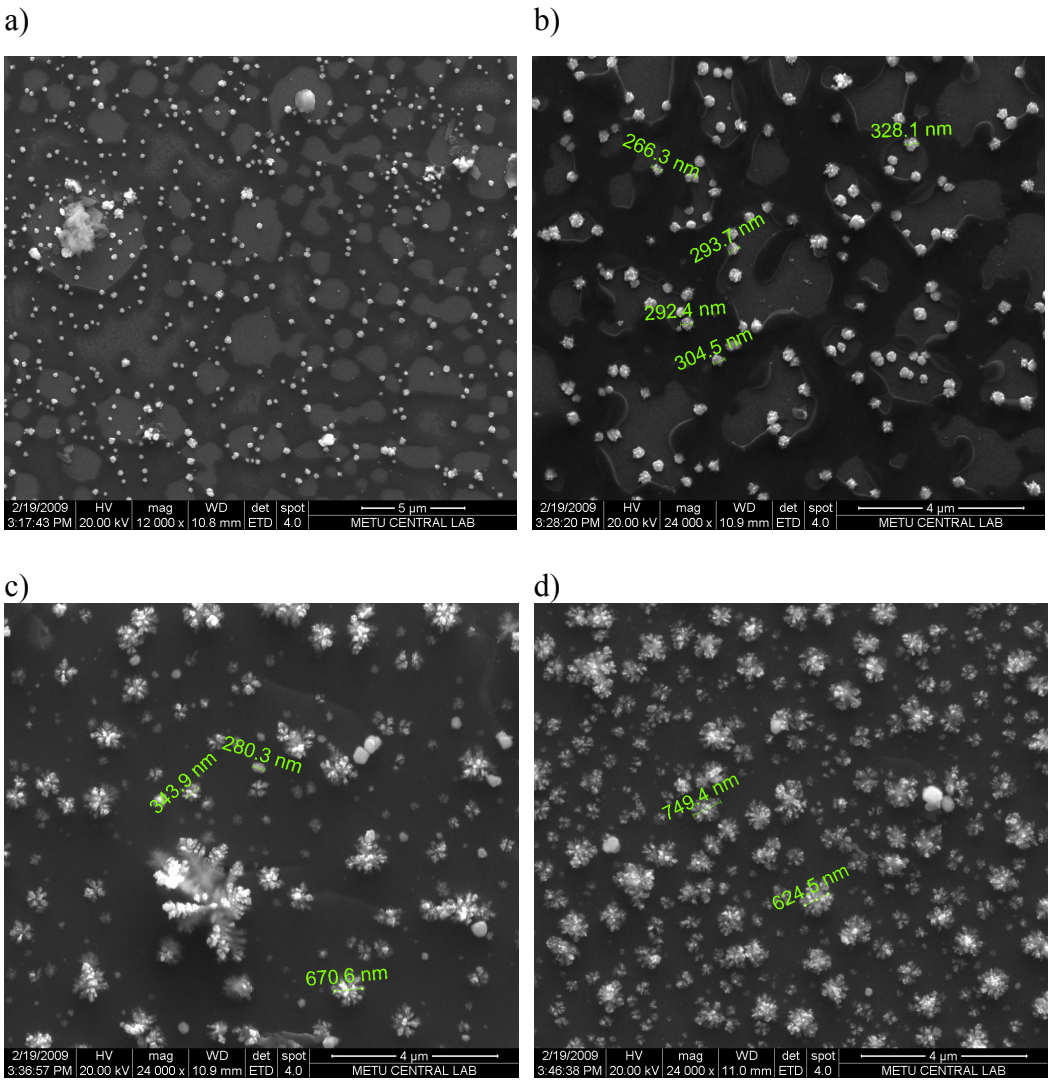

Figure 3.14. FE-SEM images of ITO-Ag substrates prepared by electrodepositing silver on ITO at various charge densities: a) 5 mC/cm^2 b) 8 mC/cm^2 c) 10 mC/cm^2 d) 15 mC/cm^2. Magnification is 24000x.

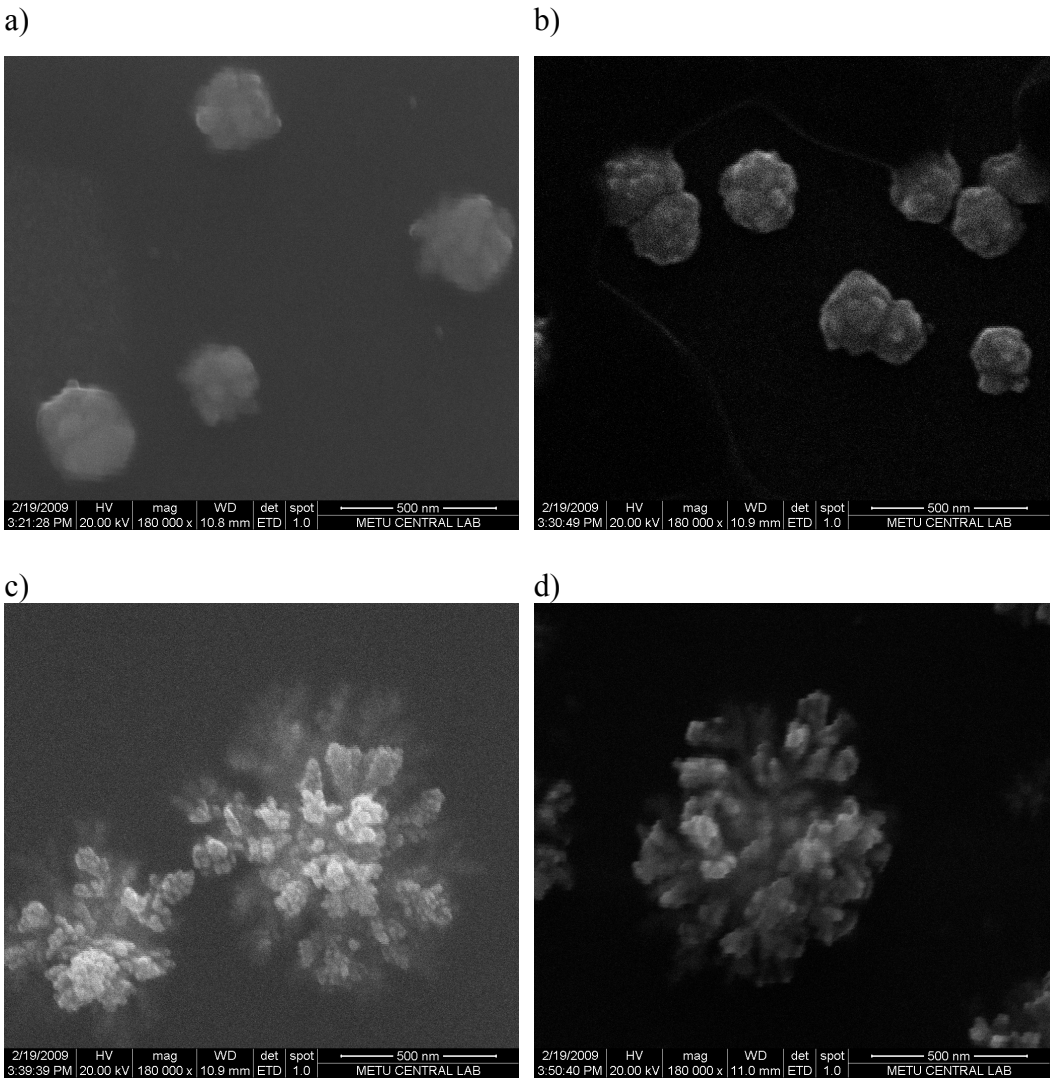

Figure 3.15. FE-SEM images of ITO-Ag substrates prepared by electrodepositing silver on ITO at various charge densities: a) 5 mC/cm^2 b) 8 mC/cm^2 c) 10 mC/cm^2 d) 15 mC/cm^2. Magnification is 180000.

3.3.1.2 The Comparison of ITO-Ag and ITO-PIII-Ag in terms of Their SERS Activities

In order to make a comparison between the performance of ITO-P**III**-Ag with that of ITO-Ag, SERS spectra of crystal Violet (CV) and para amino benzoic acid (PABA) were taken. As can be seen from Figures 3.16 and 3.17, the SERS spectra obtained with ITO-Ag are much more intense and better structured than the SERS

spectra obtained with ITO-P**III**-Ag. Peak assignments were done according to the literature values [36, 69, 70].

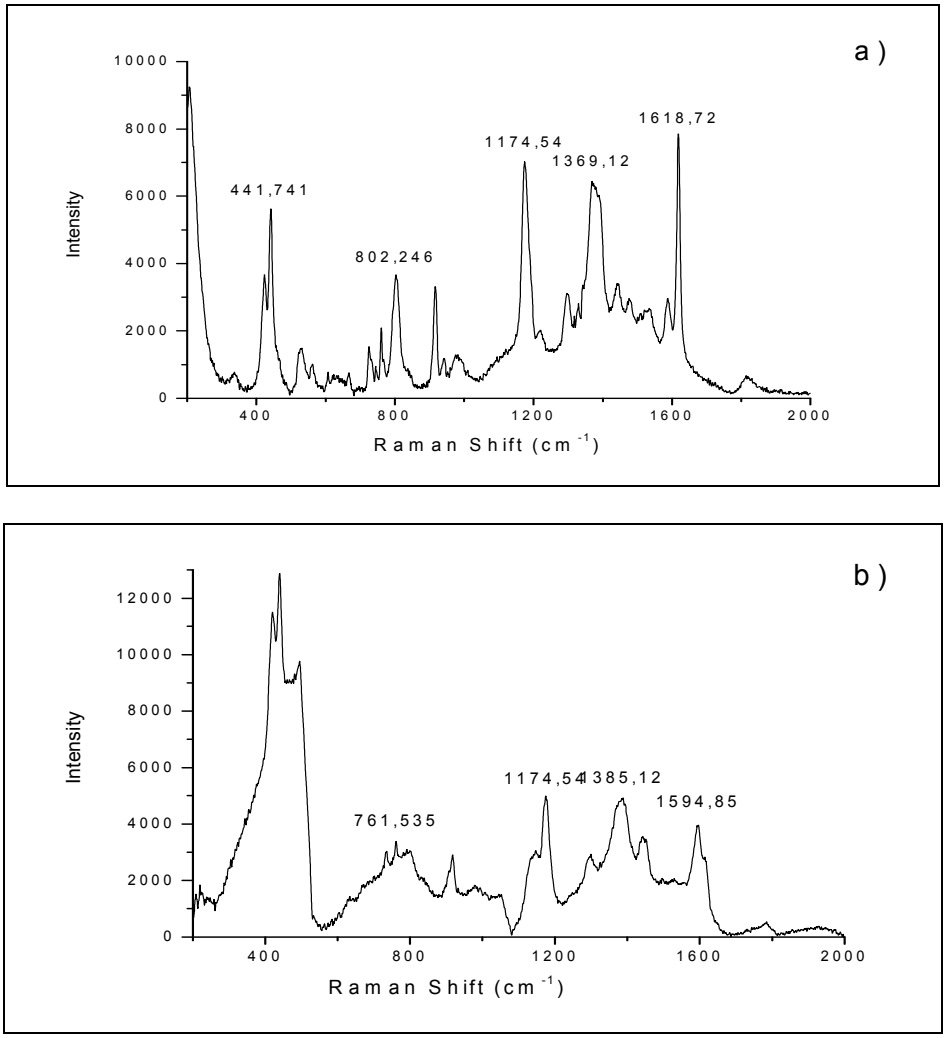

Figure 3.16. a) SERS spectrum of 10^{-5} M aqueous solution of CV obtained with ITO-Ag substrate. b) SERS spectrum of 10^{-5} M CV in acetonitrile obtained with ITO-P**III**-Ag substrate.

Table 3.9. Prominent SERS band position and assignments for CV..

CV	Peak Position (cm^{-1})	Assigment
	420, 442	ring skeletal vibration. + (C^{+}-Ph)

Table 3.9. (Continued)

CV	Peak Position (cm^{-1})	Assigment
	802	ring (C-H) bening
	913	Ring skeletal vib. of radial orientation
	1174	ring C-H bending
	1365 1384	N-Ph stretching.
	1478	ring C-C stretching + ring deformation.
	1620	ring C-C stretching.

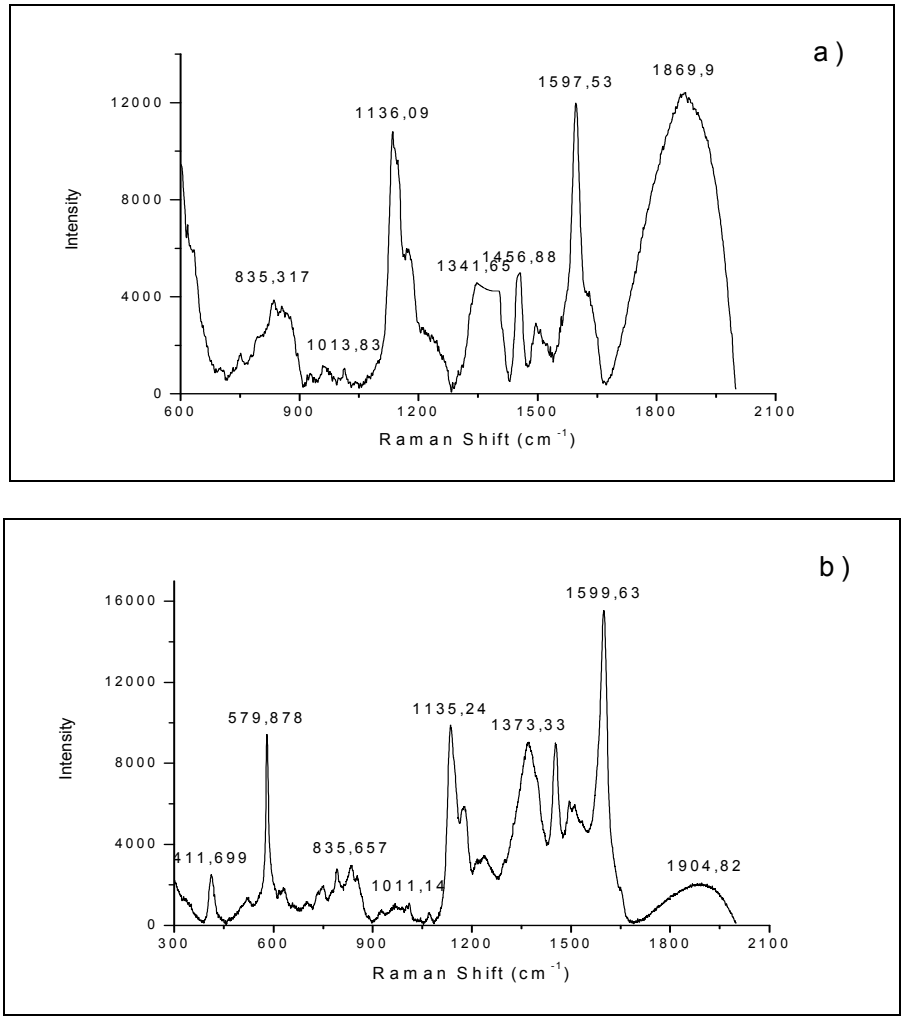

Figure 3.17. a) SERS spectrum of $5x10^{-4}$ M aqueous solution of PABA obtained with ITO-Ag substrate. b) SERS spectrum of $5x10^{-4}$ M PABA in acetonitrile solution of obtained with ITO-P**III**-Ag substrate.

Table 3.10. Prominent SERS band position and assignments for PABA.

PABA	Peak Position (cm^{-1})	Assignment
	1148	NH_2 bending
	1389	COO stretching
	1615	NH_2 stretching
	1452	Benzene ring vibration
	1515	Benzene ring vibration
	1598	Benzene ring vibration

The Raman activity of ITO-P**III**-Ag substrate was not potent enough to take the SERS spectra of $1.0x10^{-3}$ M nicotine and $4x10^{-2}$ M nicotinic acid, hence their spectra was collected by using ITO-Ag substrate only (Figure 3.18).

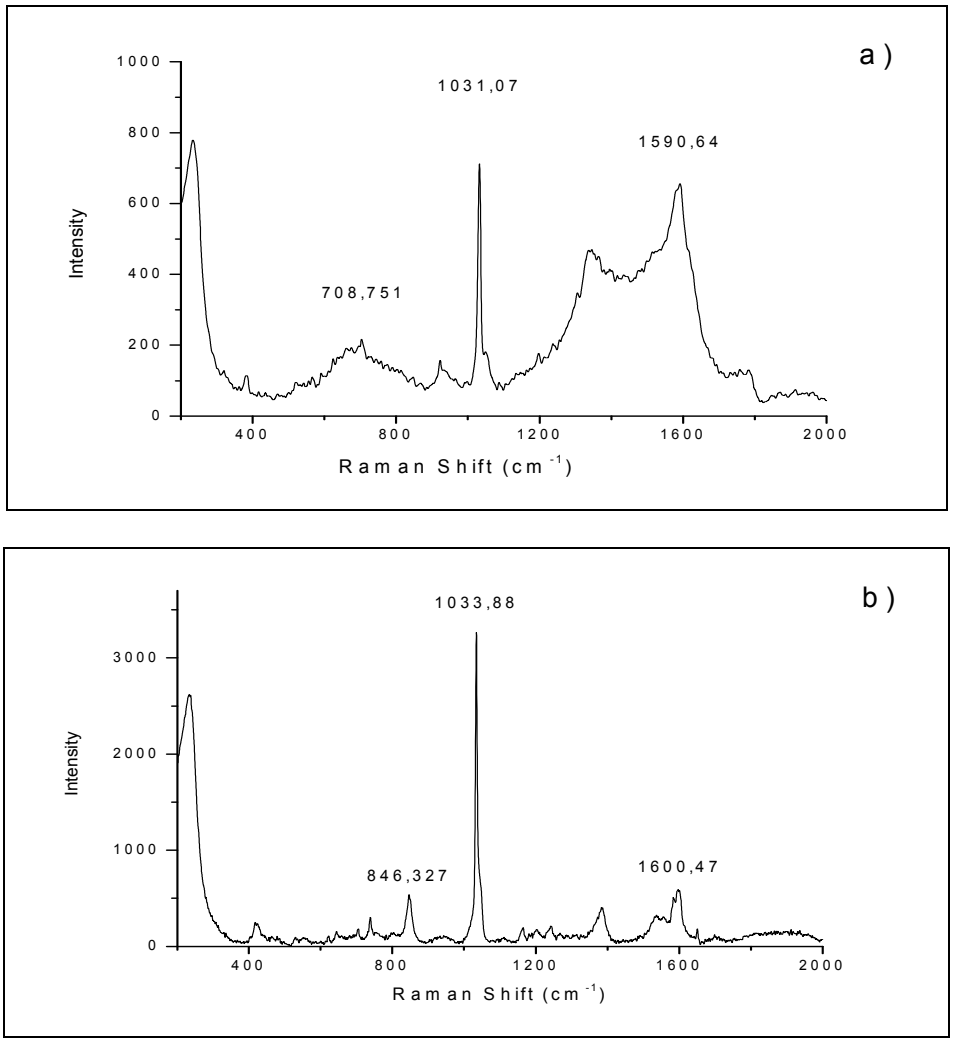

Figure 3.18. a) SERS spectrum of 10^{-3} M aqueous solution of nicotine obtained with ITO-Ag substrate. b) SERS spectrum of $4x10^{-2}$ M aqueous solution of nicotinic acid obtained with ITO-Ag substrate.

Table 3.11. Prominent SERS band position and assignments for nicotine and nicotinic Acid.

Nicotinic Acid-Nicotine	Peak Position (cm^{-1})	Assignment
	842	Ring N pyridine in Nuclei
	1032	Trigonal Ring Breathing

Table 3.11. (Continued)

Nicotinic Acid-Nicotine	Peak Position (cm^{-1})	Assignment
	1584-1604	Meta C=N plus C=C interaction effect and Asymmetric stretching of COO- group

Optimization studies for both of the substrate were carried out using 10^{-6} M BCB. In order to demonstrate the surface enhancement ability of ITO-Ag substrate and the sensitivity of SERS method, spectrum of 10^{-10} M BCB were optained.

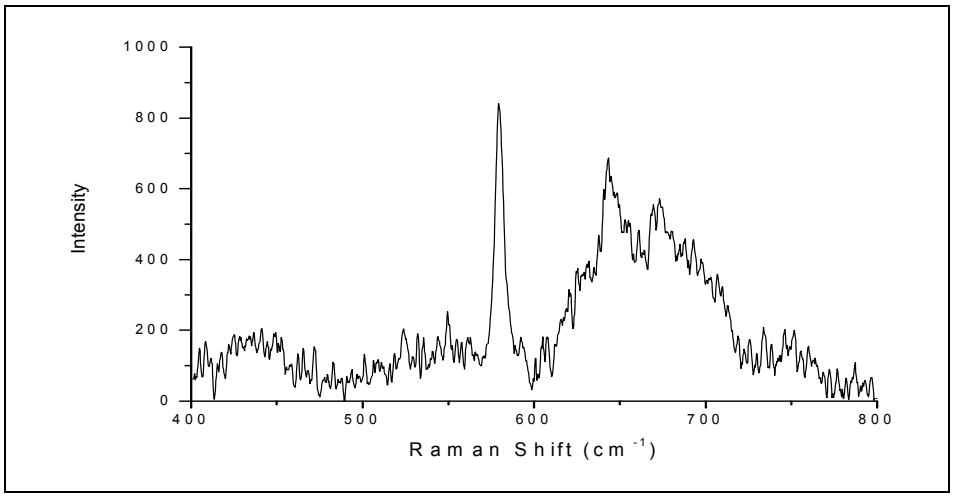

Figure 3.19. SERS spectrum of 10^{-10} M aqueous solution of BCB obtained with ITO-Ag substrate.

Table 3.12. Prominent SERS band position and assignments for BCB.

BCB	Peak Position (cm^{-1})	Assignment
	580	Benzene ring deformation mode

CHAPTER 4

CONCLUSION

In this study the usage of three cages N-polyethereal polypyrrole (P**III**) polymer synthesized through chemical and electrochemical oxidation of the M**III** in analytical studies were investigated. Chemically polymerized P**III** powders were used in the preconcentration studies of lanthanides. Whereas P**III** films, electrochemically polymerized on ITO, were used in the preparation of SERS substrates.

Chemical oxidation of the monomer (M**III**) containing polyethereal linkages has been successfully achieved yielding polymers P**III** with pseudocages. The presence of these cages makes the newly synthesized N-polyethereal polypyrrole resins an effective solid phase complexing agent for trace quantities of lanthanides. Lanthanum, europium and ytterbium ions were selected as the representative of light, medium and heavy lanthanides. High recovery values obtained at low concentrations of these ions have shown that this novel resin represents a promising material for the preconcentration of REE ions from aqueous medium over a wide pH range.

SERS-active surfaces were prepared by electrodepositing silver on P**III** coated ITO and bare ITO surfaces. The morphology (and therefore the SERS enhancement factor) of the resulting surface depends strongly on the electrochemical parameters applied during the deposition process, such as electrolyte composition, applied overpotential and cathodic charge. ITO-P**III**-Ag surfaces exhibiting the highest SERS enhancement factor were produced by using an electrolyte containing 0.05 M $AgNO_3$ in acetonitrile, a potential of -0.7 V and charge densities of 20 and 80 mC/cm^2 for polymer and silver depositions,

respectively. In the preparation of ITO-Ag substrate, silver is reduced directly on the ITO surface at a charge density of 10 mC/cm^2.

ITO-P**III**-Ag and ITO-Ag substrates were evaluated in terms of their Raman activity and the enhancement homogeneity over the surface by acquiring SERS spectra of 10^{-6} M BCB. Data were supported with FE-SEM micrograps of the substrates. Results have shown that ITO-Ag substrate show better uniformity with regard to morphology and SERS intensity over ITO-P**III**-Ag substrates. SERS spectra of crystal Violet (CV) and para amino benzoic acid (PABA) were taken utilizing these substrates in order to investigate their suitability for the determinations of organic compounds. The high sensitivity, particularly achieved with ITO-Ag substrates. It is desirable to carry out further investigations into the morphology and size of the nanoparticles introduced on the surfaces electrochemically and more indepth study into what limits the homogeneous nucleation and growth of these particles and thereby affects the SERS activity of these surfaces.

REFERENCES

[1]- Cihaner, A. *J. Macromol. Sci. Pure Appl. Chem.* **2006**, 43, 1379.

[2]- Simonet, J.; Gache, Y.; Simonet-Gueguen, N.; Leclerc, O. *Denki Kagaku* **1994**, 62, 1211.

[3]- Algı, F.; Cihaner, A. *Tetrahedron Lett*. **2008**, 49, 3530.

[4]- Bartlett, P. N.; Benniston, A. C.; Chung, L.-Y.; Dawson, D. H.; Moore, P. *Electrochim. Acta* **1991**, 36, 1377.

[5]- Youssoufi, H. K.; Hmyene, M.; Garnieri, F.; Delabouglise, D. *J. Chem. Soc. Chem. Commun*. **1993**, 1550.

[6]- Cihaner, A. *J. Electroanal. Chem.* **2007**, 605, 8.

[7]- Topp, N. E. "The Chemistry of The REEs", Elsevier Publishing Company, Amsterdam, London, New York, 1965.

[8]- Chemistry.about, http://chemistry.about.com/od/elementgroups/a/rareearths.htm last accessed 2.12.2008.

[9]- Wu, S.; He, M.; Hu, B.; Jiang, Z. *Microchim. Acta* **2007**, 159, 269.

[10]- Rao T.; Kala R.; *Talanta* **2004**, 63, 949.

[11]- Xu, Z.; Liu, C.; Zhang, H.; Ma, Y.; Lin, S. *Anal. Sci*. **2003**, 19, 1625.

[12]- Agrawal, Y. K. *Fullerenes, Nanotubes, and Carbon Nanostructures* **2007**, 12, 545.

[13]- Taicheng, D.; Hangting, C.; Xianjin, Z. *J. Anal. At Spectrom.* **2002**, 17, 410.

[14]- Agrawal, Y. K. *Fullerenes, Nanotubes, and Carbon Nanostructures*, **2007**, 15, 353.

[15]- Fu, Q.; Yang, L.; Wang, Q. *Talanta* **2007**, 72, 1248.

[16]- Chen, S.; Xiao, M.; Dengbo, L.; Zhan, X. *Anal.l Lett.* **2007**, 40, 2105.

[17]- Sabarudin, A.; Lenghor, N.; Oshima, M.; Hakim, L.; Takayanagi, L.; Gao, Y.; Motomizu, S. *Talanta* **2007**, 72, 1609.

[18]- Helfferich, F. G. "Ion Exchange, McGraw Hill", New York, 1962.

[19]- Rimskaya-Korsakova, M. N.; Dubinin, A. V.; Ivanov V. M. *J. Anal. Chem.* **2003**, 58, 870.

[20]- Pasinli, T.; Eroğlu, A. E.; Shahwan, T. *Anal. Chim. Acta* **2005**, 547, 42.

[21]- Kong, X.; Jia, Q.; Zhou W. *Microchem. J.* **2007**, 87, 132.

[22]- Figueiredo, A. M. G.; Avristcher, W.; Masini, E. A.; Diniz, S. C.; Abrao, A. *J. Alloys Comp.* **2002**, 344, 36.

[23]- Minowa, H.; Ebihara, M. *Anal. Chim. Acta* **2003**, 498, 25.

[24]- Shaw, T. J.; Duncan, T.; Schnetger, B. *Anal. Chem.* **2003**, 75, 3396.

[25]- Chen, S.; Xiao, M.; Dengbo, L.; Zhan, X. *Anal. Lett.* **2007**, 40, 2105.

[26]- Skoog, D. A.; James, J. J.; "Principles of Instrumental Analysis", Saunders College Publishing, USA, 1992.

[27]- Stefánsson, A.; Gunnarsson, I.; Giroud, N. *Analytica Chimica Acta* **2007**, 582, 69.

[28]- Mermet, J. M. *J. Anal. At. Spectrom.* **2005**, 20, 11.

[29]- Cai, B.; Hu, B.; Xiong, H.; Liao, Z.; Mao, L.; Jiang, Z. *Talanta* **2001**, 55, 85.

[30]- Liang, P.; Chen, X. *Anal. Sci.* **2005**, 21, 1185.

[31]- Hang, Y.; Qin, Y.; Shen, J. *J. Sep. Sci.* **2003**, 26, 957.

[32]- Liang, P.; Cao, J.; Liu, R.; Liu, Y. *Microchim. Acta* **2007**, 159, 35.

[33]- Fleishmann, M.; Hendra, P.; McQuillan, A. *Chem. Phys. Lett*. **1974**, 26 163.

[34]- Zhang, X.; Yonzon, C. R.; Young, M. A.; Stuart D. A.; Van Duyne, R.P. *IEE Proc. Nanobiotechnology* **2005**, 152, 195.

[35]- Kudelski, A. *Chem. Phys. Lett.* **2005**, 414, 271.

[36]- Karabıçak, S.; Kaya, M.; Vo-Dinh, T.; Volkan M. *J. Nanosci. Nanotech.* **2008**, 8, 955.

[37]- Tripp, R. A.; Dluhy, R. A.; Zhao, Y. *Nanotoday* **2008**, 3, 31.

[38]- Aroca, R. Surface-Enhanced Vibrational Spectroscopy; John Wiley & Sons: Chichester, U.K., **2006**.

[39]- Sanchez-Cortes, S.; Garcia-Ramos, J. V. *J. Raman Spect.* **1998**, 29, 365.

[40]- Pieczonka, N.; Aroca, R. *Chem. Phys. Chem.* **2005**, 6, 2473.

[41]- Zhang, A.; Tie, X.; Zhang, J.; An, Y.; Li, L. *Appl. Surf. Sci.* **2008** 255, 3184.

[42]- Jerez-Rozo, J. I.; Primera-Pedrozo, O. M., Barreto-Cabán, M. A.; Hernández-Rivera, S. P. *IEEE Sensors Journal* **2008**, 8, 974.

[43]- House P. G.; Schnitzer C. S. *J. Coll. Inter. Sci.* **2008**, 318, 145.

[44]- Tantra, R.; Brown, R. J. C.; Milton, M. J. T. *J. Raman Spect.* **2007**, 38, 1469.

[45]- Tiwari, V. S.; Oleg, T.; Darbha, G. K.; Hardy, W.; Singh, J. P.; Ray P. C. *Chem. Phys. Lett.* **2007**, 446, 77.

[46]- Green, M.; Liu, F. M. *J. Phys. Chem. B* **2003,** 107*,* 13015.

[47]- Li, P.-W.; Zhang, J.; Zhang, L.; Mo, Y.-J. *Vibrational Spectroscopy* **2009**, 49, 2.

[48]- Stöckle, R. M.; Deckert, V.; Fokas, C.; Zenobi, R. *Appl. Spectrosc.* **2000**, 54, 1577.

[49]- Stokes, D. L.; Vo-Dinh, T. *Sensors and Actuators B* **2000**, 69, 28.

[50]- Litorja, M.; Haynes, C. L.; Haes, A. J.; Jensen, T. R.; Van Duyne, R. P. *J. Phys. Chem. B* **2001,** 105, 6907.

[51]- Zhang, X.; Zhao, J. ; Alyson, V.; Jeffrey, W.; Elam, W.; Van Duyne, R. P. *J. Am. Chem. Soc.* **2006**, 128, 10304.

[52]- Kim, K.; Lee, H. B.; Park, H. K.; Shin K.S. *J. Coll. Inter. Sci.* **2008**, 318 ,195.

[53]- Lin, W.-C.; Yang, M.-C. *Macromole. Rapid Commun.* **2005**, 26, 1942.

[54]- Hasell,T.; Lagonigro, L.; Peacock, A. C.; Yoda, S.; Brown, P. D.; Sazio, P. J. A.; Howdle, S. M. *Adv. Funct. Mater.* ***200*8**, 1265.

[55]- Lu, J.; Chamberlin, D.; Rider, D.A.; Liu, M.; Manners, I.; Russel, T.P. *Nanotechnology* **2006**, 17 ,5792.

[56]- Wang, C.C.; Chen, J.S. *Electrochim. Acta* **2008**, 53, 5615.

[57]- Wang , C.-C. *J. Phys. Chem. C* **2008,** *112,* 5573.

[58]- Tourwe, E.; Hubin, A. *Vibrational Spectroscopy* **2006**, 41, 59.

[59]- Geddes, C. D.; Parfenov, A.; Roll, D.; Fang, J.; Lakowicz , J. R. *Langmuir*, **2003**, 19 (15), 6236.

[60]- Liu, Y.-C.; Yu, C.-C.; Hsu, T.-C. *J. Phys. Chem. C*, **2008**, 112 (41), 16022.

[61]- Sauer, G.; Nickel, U.; Schneider, S. *J. Raman Spect.* **2000**, 31, 359.

[62]- Leclerc, O. **1997,** *United States Patent,* No5644064.

[63]- Kruszewski, S.; Kobiela, T. *Vacuum* **1999,** 54, 245.

[64]-. Tian, Z.-Q.; Ren, B. *Annu. Rev. Phys. Chem.* **2004,** 55, 197.

[65]- Bilmes, S. *J. Chem. Soc. Faraday Trans.* **1996,** 92, 2381.

[66]- Fransaer, J.; Penner, R. *J. Phys. Chem. B* **1999,** 103, 7643.

[67]- Penner, R.M. *J. Phys. Chem. B* **2001,** 105, 8672.

[68]- Sandmann, G.; Dietz, H.; Plieth, W. *J. Electroanal. Chem.* **2000,** 491, 78.

[69]- Persaud, I.; Grossman, W. *J.Raman Spect.* **1993,** 24, 107.

[70]- Lueck, B.; Daniel C.; McHale L. *J. Raman Spect.* **1993**, 24, 363.